AD-A055 380 AIR FORCE FLIGHT DYNAMICS LAB WRIGHT-PATTERSON AFB OHIO F/G 1/2
THE EFFECTS OF WIND SHEAR ON AUTOMATIC LANDING.(U)
APR 77 R P DENARO

UNCLASSIFIED AFFDL-TR-77-14 NL

1 OF 1
ADA
055380

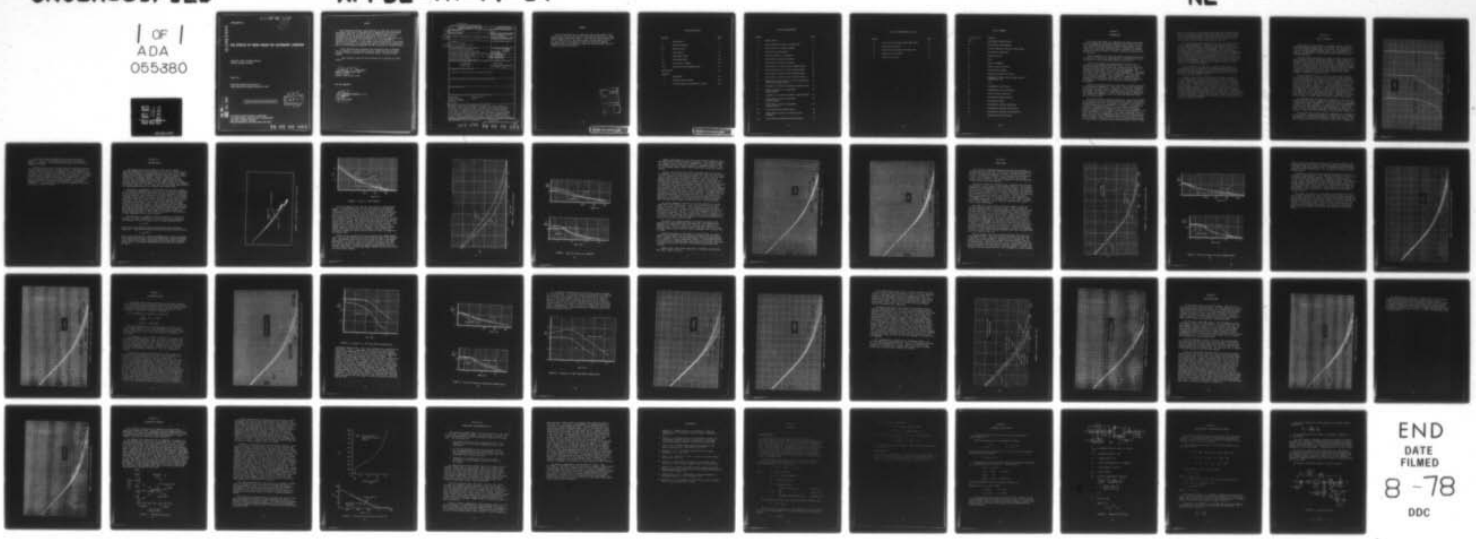

END
DATE FILMED
8-78
DDC

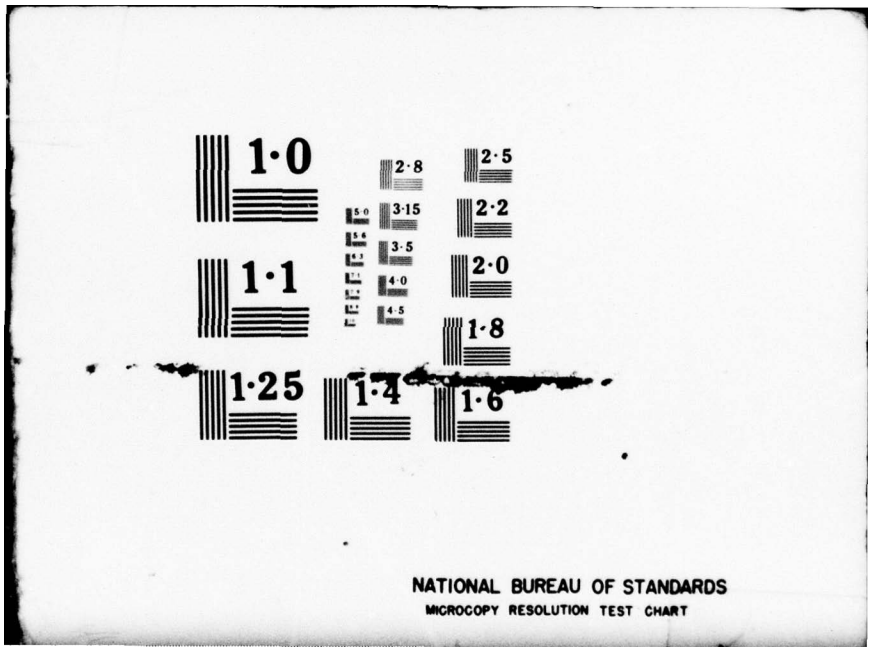
1·0
1·1
1·25
1·4
1·6
1·8
2·0
2·2
2·5
2·8
3·15
3·5
4·0
4·5
5·0
NATIONAL BUREAU OF STANDARDS
MICROCOPY RESOLUTION TEST CHART

AFFDL-TR-77-14

THE EFFECTS OF WIND SHEAR ON AUTOMATIC LANDING

TERMINAL AREA CONTROL BRANCH
FLIGHT CONTROL DIVISION

APRIL 1977

TECHNICAL REPORT AFFDL-TR-77-14
FINAL REPORT FOR PERIOD ENDING MAY 1976

AIR FORCE FLIGHT DYNAMICS LABORATORY
AIR FORCE WRIGHT AERONAUTICAL LABORATORIES
AIR FORCE SYSTEMS COMMAND
WRIGHT-PATTERSON AIR FORCE BASE, OHIO 45433

NOTICE

When Government drawings, specifications, or other data are used for any purpose other than in connection with a definitely related Government procurement operation, the United States Government thereby incurs no responsibility nor any obligation whatsoever; and the fact that the Government may have formulated, furnished, or in any way supplied the said drawings, specifications, or other data, is not to be regarded by implication or otherwise as in any manner licensing the holder or any other person or corporation, or conveying any rights or permission to manufacture, use, or sell any patented invention that may in any way be related thereto.

This report has been reviewed by the Information Office (ASD/OIP) and is releasable to the National Technical Information Service (NTIS). At NTIS it will be available to the general public, including foreign nations.

This technical report has been reviewed and is approved for publication.

Robert P. Denaro

ROBERT P. DENARO, Capt, USAF
Project Engineer
Terminal Area Control Branch

FOR THE COMMANDER

R P Johannes

R. P. JOHANNES
Acting Chief
Flight Control Division

AIR FORCE - 28 JUN 77 - 300

UNCLASSIFIED

SECURITY CLASSIFICATION OF THIS PAGE *(When Data Entered)*

REPORT DOCUMENTATION PAGE

READ INSTRUCTIONS BEFORE COMPLETING FORM

1. REPORT NUMBER: AFFDL-TR- 77-14	2. GOVT ACCESSION NO.
3. RECIPIENT'S CATALOG NUMBER	
4. TITLE *(and Subtitle)*: The Effects of Wind Shear on Automatic Landing.	5. TYPE OF REPORT & PERIOD COVERED: Final Report for Period Ending May 1976
	6. PERFORMING ORG. REPORT NUMBER
7. AUTHOR(s): Robert P. Denaro, Capt, USAF	8. CONTRACT OR GRANT NUMBER(s)
9. PERFORMING ORGANIZATION NAME AND ADDRESS: Terminal Area Control Branch, Air Force Flight Dynamics Laboratory, Wright-Patterson Air Force Base, Ohio 45433	10. PROGRAM ELEMENT, PROJECT, TASK AREA & WORK UNIT NUMBERS: 62201F, 82260140
11. CONTROLLING OFFICE NAME AND ADDRESS: Air Force Flight Dynamics Laboratory (FGT), Air Force Systems Command, Wright-Patterson AFB, Ohio 45433	12. REPORT DATE: April 1977
	13. NUMBER OF PAGES: 45
14. MONITORING AGENCY NAME & ADDRESS *(if different from Controlling Office)*: 53p.	15. SECURITY CLASS. *(of this report)*: UNCLASSIFIED
	15a. DECLASSIFICATION/DOWNGRADING SCHEDULE: N/A

16. DISTRIBUTION STATEMENT *(of this Report)*

Approved for public release; distribution unlimited.

17. DISTRIBUTION STATEMENT *(of the abstract entered in Block 20, if different from Report)*

18. SUPPLEMENTARY NOTES

19. KEY WORDS *(Continue on reverse side if necessary and identify by block number)*

Wind Shear
Wind Disturbance
Automatic Landing
Autoland
Automatic Flare
Flare

20. ABSTRACT *(Continue on reverse side if necessary and identify by block number)*

Automatic approaches and landings are simulated on a hybrid computer in constant winds, linear wind shear, logarithmic wind shear and knife-edge wind shear to determine the effects of wind shear on automatic landing. The aircraft is modeled by the longitudinal equations of a large jet transport with a typical autoland system. Results identified large differences in performance in the three types of shear, with large touchdown dispersions in moderate logarithmic wind shears. Analysis indicated that performance in logarithmic wind shear was strongly dependent on airspeed deviations.

DD FORM 1 JAN 73 1473 EDITION OF 1 NOV 65 IS OBSOLETE

UNCLASSIFIED

SECURITY CLASSIFICATION OF THIS PAGE *(When Data Entered)*

FOREWORD

The work described in this report was done by the author in the Terminal Area Control Branch of the Flight Control Division, Air Force Flight Dynamics Laboratory (AFFDL). The study came under Project 8226, Task 01, Work Unit 40. The author extends sincere appreciation to Mr. Butch Foley of the 4950th Test Wing for the hybrid computer programming and Captain Bohdan G. Kunciw and Captain Thomas Imrich of AFFDL for analysis consultation.

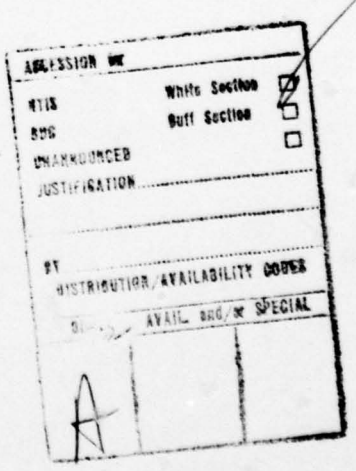

TABLE OF CONTENTS

LIST OF ILLUSTRATIONS

LIST OF ILLUSTRATIONS (cont'd)

LIST OF SYMBOLS

a, b, C, h_o, K	Constants
GPIP	Glide path intercept point
h	Wheel height above ground
$\dot{h}$	Vertical speed or sink rate (earth frame)
M_i	Pitch force coefficient
q	Dynamic pressure
t	Time
t_f	Time at touchdown
t_o	Time at flare initiation
u	Perturbation airspeed
V	Reference airspeed, 262 ft/sec
V_w	Component of wind velocity along aircraft longitudinal axis
w	$= V\alpha$
$\ddot{x}$	Longitudinal acceleration
X_w	Longitudinal force coefficient
Z_w	Vertical force coefficient
α	Perturbation angle-of-attack
ΔT	Perturbation thrust
δe	Perturbation elevator deflection
δs	Perturbation stabilizer deflection
δ_T	Perturbation throttle lever position
θ	Perturbation pitch attitude

SECTION I

INTRODUCTION

The initial motivation for conducting this study of wind shear effects on automatic landing was generated from observation of aircraft performance during automatic landing flight testing. During some tests, the aircraft terminated flare by "floating" in ground effect two or three feet above the runway. Sometimes the aircraft rotated too quickly at flare initiation, requiring corrective action by the pilot.

Another abnormal test result had opposite symptoms during flare. In these cases, the aircraft appeared not to rotate enough at flare initiation, or even pitched down slightly during flare.

Analysis of airspeed and groundspeed histories for these particular flights showed interesting trends. In most cases, the floating condition described above was accompanied by an increase in airspeed near the ground, with a decrease in groundspeed, thus indicating a rather rapid increase in headwind component. The second condition, diving during flare, was often accompanied by a rapid loss of airspeed, with a slight gain in groundspeed. This indicates a loss of headwind component. These changes in longitudinal wind component were attributed to wind shear, and a computer simulation was designed to investigate these trends in a more controlled environment.

Before discussing the results of the study, an intuitive analysis of the problem is appropriate. Wind effects on aircraft landing can be logically separated into two categories: effects due to steady-state winds, and effects due to changing winds. For the purposes of this report, any reference to "wind", unless otherwise stated, means the longitudinal component of the wind along the forward velocity vector of the aircraft.

An aircraft flying at a given airspeed in a steady-state headwind or tailwind will have a groundspeed that differs from its airspeed by the magnitude of the wind. For example, an airspeed of 150 knots in a 30 knot headwind yields a groundspeed of 120 knots. Since approach airspeed is dictated primarily by aircraft configuration and is relatively independent of steady-state wind velocity, groundspeed during the approach will be largely a function of wind velocity. Also, since the aircraft is constrained to fly along a glidepath fixed in space, there will be a proportional change in vertical speed and power. These variations create few problems until flare, the last 40 to 70 feet of altitude. Flare involves a critical transition from primarily air-based motion to primarily ground-referenced motion, that is, from

flying to ground roll. The desired final conditions remain unchanged; there is a specified vertical speed at touchdown and a desired touchdown distance down the runway. With vertical and horizontal speeds at flare initiation varying due to wind, the control required to bring the aircraft to these fixed final conditions will vary.

The second category of wind effects, that due to changing winds, causes further complications. Because of an aircraft's mass and inertia, and sensor delays, a change in wind speed will take a period of time to change the aircraft's groundspeed. Thus, an aircraft attempting to hold an approach airspeed might lose or gain airspeed in a wind shear, with the severity of the condition partially dependent on the magnitude of the wind shear and speed with which it occurs. This airspeed change can affect aerodynamic forces on the aircraft and control effectiveness for maneuvering, possibly causing serious control problems during landing. This is particularly true when the flight control is performed by autopilot, since autopilot gains are usually selected for one aircraft airspeed.

These two effects of winds, due to constant winds and due to changing winds, have varying levels of dominance depending on wind magnitude, type of wind shear, and certain aircraft characteristics. References are made throughout this discussion to these factors and how they affect the landing parameters.

Evidence of the reality of the wind shear problem for normal aircraft operations is illustrated by recent aircraft incidents. On 4 January 1971, nine consecutive aircraft executed missed approaches to runway 04R at Kennedy International Airport, NY, due to touchdown point overshoots. Measurements confirmed the existence of a tailwind decreasing with altitude at a rate of about 20 kts/100 ft (Ref 4). Another notable wind shear incident involved a fatal DC-10 accident at Boston's Logan International Airport on 17 December 1973. The details of the wind shear and aircraft performance are discussed in the discussion section of this report. These cases, as well as many recent suspected wind shear accidents, dramatically illustrate the need for research into wind shear effects on landing.

SECTION II

SCOPE OF RESEARCH

The objective of this study was to compare automatic landing performance under different types of wind shear and to identify the cause of performance degradations in each case. The parameter of interest was longitudinal touchdown point. Vertical speed at touchdown was considered when it contributed further insight into the landing performance.

The main comparison studied was between two types of shear models which followed linear and logarithmic profiles. Linear models of 8 kts/100 ft are used by the FAA for Category II, Category IIIA, and Automatic Landing System certification criteria in Advisory Circulars 120-29, 120-28A, and 20-57A. The military does not address wind shear at all in the Handling Qualities Military Specification, MIL-F-8785B. In contrast to these specifications, many recent meteorological studies have shown that average wind shear profiles more closely resemble a logarithmic curve (Ref 3, 9).

The most probable reason for the use of linear shear profiles for certification is the nature of pilot reports of shear intensity. A pilot can determine, for example, a loss of 8 knots airspeed from an altitude of 200 feet AGL to 100 feet AGL, and report this as a wind shear of 8 kts/100 ft. This format is fine for estimating expected values of wind shear. However, it is not necessarily an accurate indication of what the wind shear value was from 300 feet to 200 feet or from 100 feet to the ground. In other words, the apparently linear wind shear that a pilot notices from 200 feet to 100 feet might only be a segment of a total logarithmic wind shear. Regardless of the cause for the use of linear wind shear models, it appears to be worthwhile to compare autoland response to the two types of wind shears.

The wind model used for logarithmic wind shear is similar to the neutral stability case for atmospheric conditions (Ref 3). This model is developed in detail in Appendix A. The linear shear was programmed to begin at the same altitude as the logarithmic shear and decrease or increase by the same magnitude in comparative cases. A third wind shear, called a "knife-edge" shear, was a smoothed step change in wind velocity. Profiles of these wind models are illustrated in Figure 1.

The autoland flare system chosen for simulation was an exponential $\dot{h}$ flare system. Although technically not a state-of-the-art system, it did represent an off-the-shelf example of current flare systems. The flare law and system design are discussed in more detail in Appendix B.

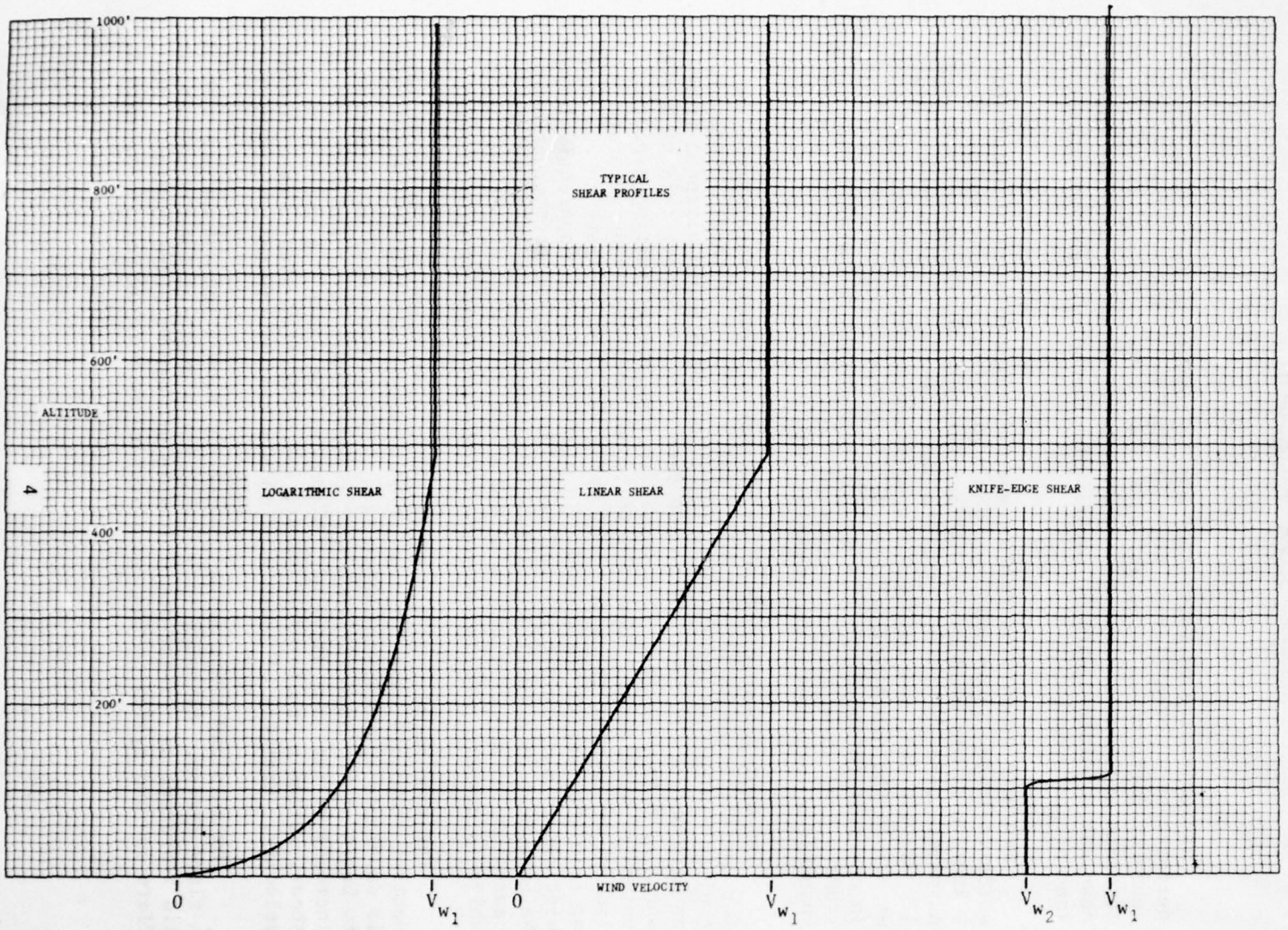

FIGURE 1. Wind Profiles

The aircraft model and autothrottle system are described in Appendix C. The aircraft modeled was an Air Force KC-135A four-engine jet transport. The simulation modeled only the longitudinal equations of motion.

Simulated shear cases are analyzed first with headwind conditions, the most likely encounter for a landing aircraft. The comparison of tailwind cases with no wind cases, however, is usually somewhat easier to analyze. Both analyses are included for each shear type. In general, the discussion will compare wind shear condition landings to a no-wind condition, both of which are referenced to a nominal case. Nominal, as it is used here, refers to the profile defined by the flare law equations which do not consider aircraft dynamics or atmospheric disturbances. It is the profile that would be commanded by the flare system under no-wind conditions.

SECTION III

CONSTANT WINDS

The simplest type of wind condition is one with a constant magnitude throughout the entire descent of the aircraft. These constant winds affect primarily the groundspeed and initial conditions at flare. Because airspeed remains unchanged, aircraft response to control surface deflection is relatively constant. Therefore, response delays to initial flare law commands remain the same. These response delays normally cause an initial error between the computed flare law flight path and the actual profile flown. If the initial conditions are changed by constant winds, this initial flare error will be changed, and ultimately the landing performance will be different than without winds.

The analysis of headwind or tailwind effect on autoland performance is facilitated by comparing these cases with a "no-wind" case. Regardless of the winds present, the aircraft will overshoot the nominal flare path, since the automatic flare system must see an error before it can generate a command to the elevator to close out the error. In the case of a headwind, the aircraft has a lower initial sink rate than in no-wind at flare initiation. This results in less of a flare law (nominal flare path) overshoot than that which occurs in the no-wind case, and the system closes out the error more quickly. Figure 2 demonstrates this reduction in flare law overshoot, as shown by the headwind flight path starting out above the no-wind flight path. Later, during the final seconds of flare, the headwind flight path descends through the no-wind case and lands shorter, shown in Figure 3. This is due to the nature of the flare law, aircraft groundspeed, and aircraft airspeed.

The flare law is a schedule of vertical velocity as a function of altitude. As shown in Appendix B, if the aircraft flares according to this schedule, the vertical velocity will be reduced exponentially, or

$$\dot{h} = C_1 e^{-at}$$

where C and a are constants determined by desired initial and final conditions. Integrating the above expression yields the altitude profile:

$$h = C_2 e^{-at} + b$$

where b can be adjusted for a desired touchdown bias. Since this profile is a function only of time, range covered during flare varies with groundspeed. While the altitude is governed by the vertical velocity schedule, forward motion is governed by groundspeed which includes the influence of winds.

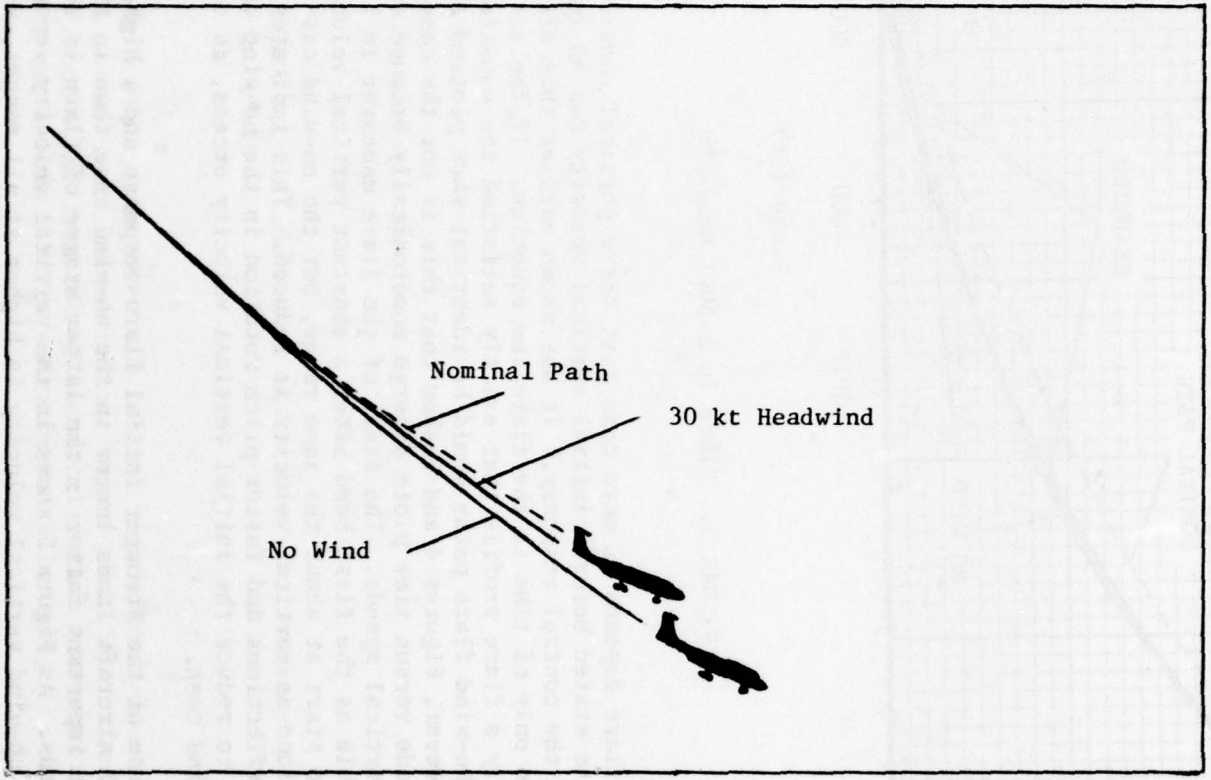

FIGURE 2. Initial Headwind Effects on Flight Path

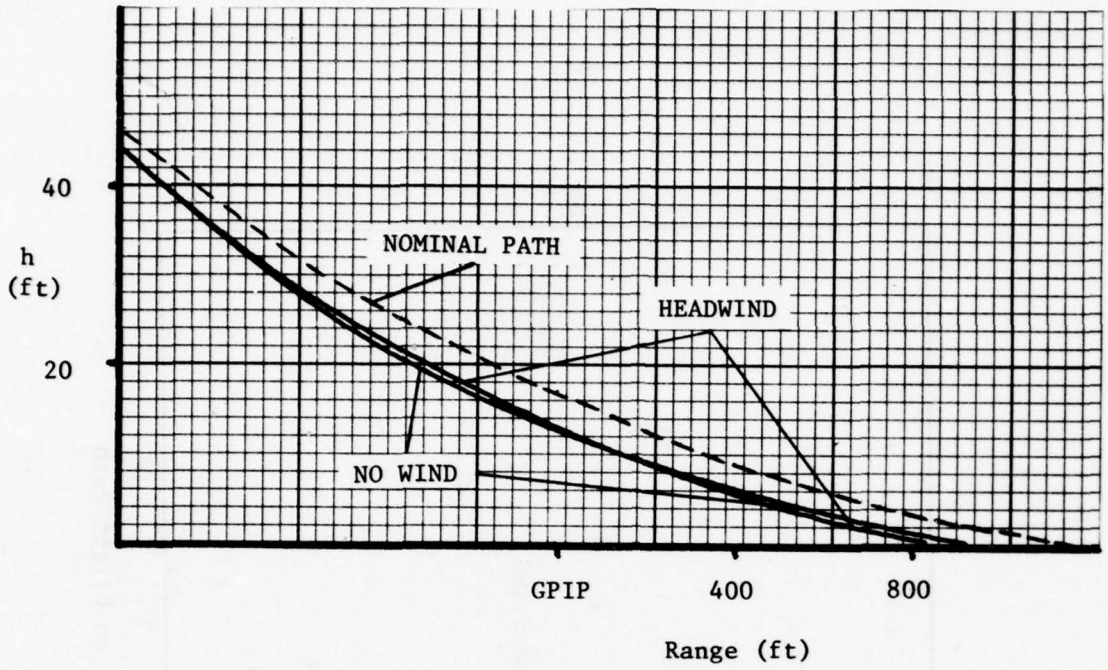

FIGURE 3. Flare In A 30KT Headwind

The flare depends on more than just these physical considerations, though. As stated before, initial vertical velocity has an important effect on the control response. It was shown earlier that altitude is a function only of time in the flare law equation. If the aircraft were able to fly a flare profile that exactly satisfied the equation, headwind and no-wind flare paths would be identical when plotted against time. However, Figures 4 and 5 show that this is not the case. At first the altitude versus time plots diverge monotonically because of different initial vertical speeds. The start of the flare maneuver in Figure 5 is identifiable as the first bend after a constant vertical velocity. Flare appears to start at about the same range, but the no-wind case has a steeper slope as vertical velocity is reduced. This indicates greater control deflections and faster pitch rotation in the no-wind case, necessary to reduce the initial vertical velocity excess, as compared to the headwind case.

Because of the stronger initial flare response and a higher groundspeed, the aircraft lands longer in the no-wind case than in the headwind case. The important factor in the latter stages of flare is the higher groundspeeds. As Figure 5 shows in the vertical velocity versus range plot, the no-wind vertical velocity is higher at all ranges, yet the aircraft lands longer. Without the higher groundspeed in no-wind, the altitude covered with this sustained higher vertical velocity would result in a much shorter landing.

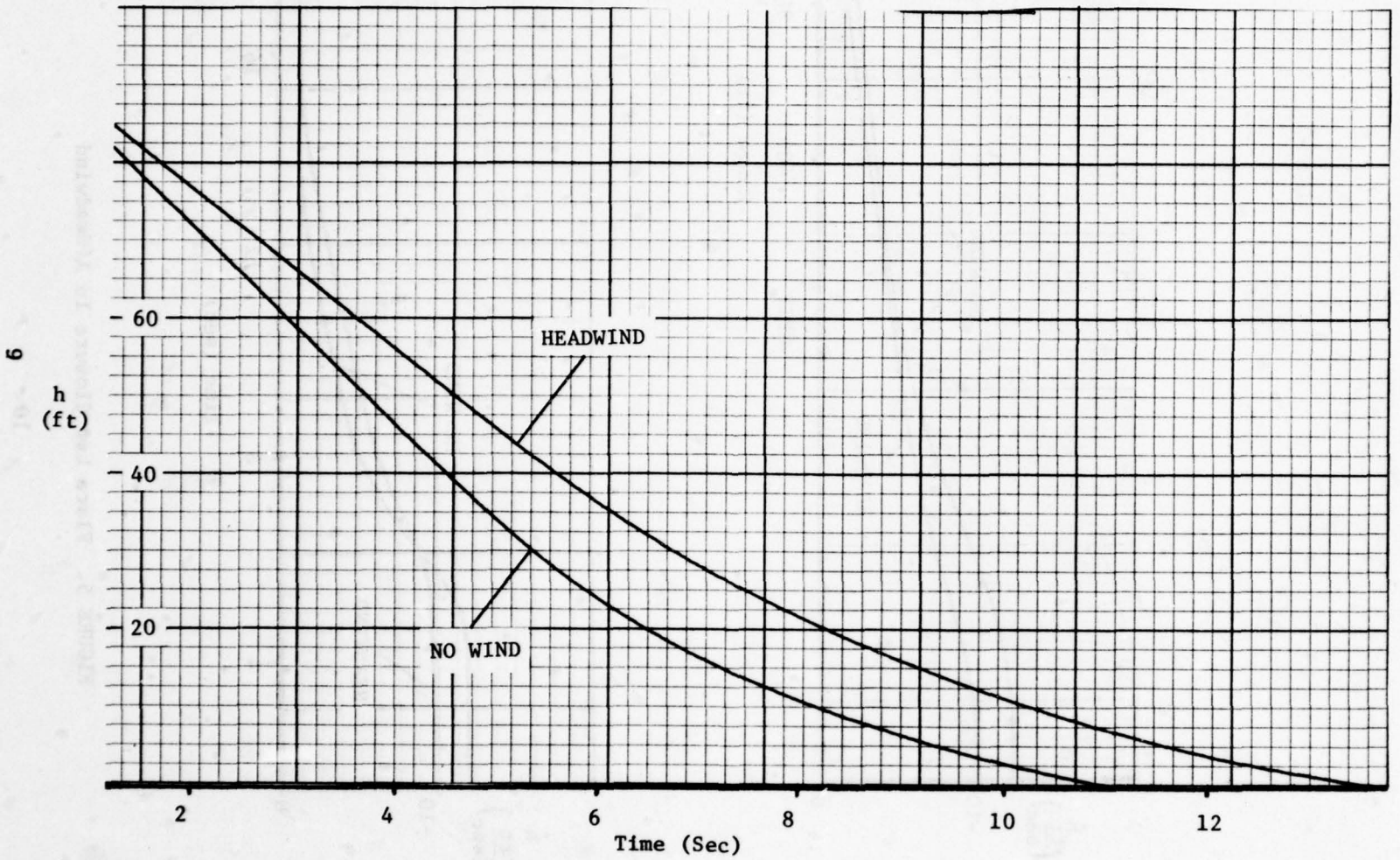

FIGURE 4. Flare Path In Time Domain

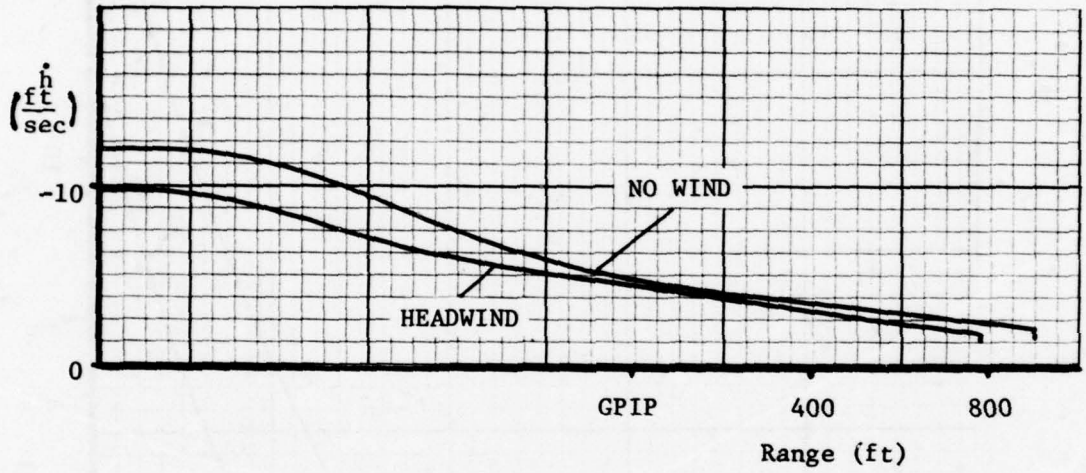

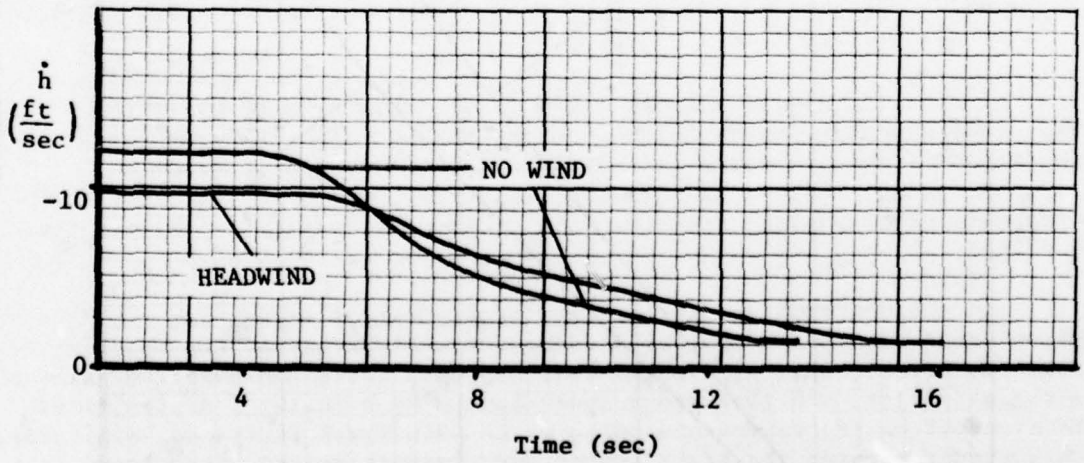

FIGURE 5. Flare Law Closure In A Headwind

Another consideration in this case is the airspeed response to the open loop throttle retard described in Appendix C. Since throttle retard is a function only of time, and the headwind case takes longer to land, the airspeed loss due to throttle retard in a headwind is greater. The loss of airspeed reduces control effectiveness and re-enforces a shorter landing.

Besides these three factors, there is another effect due to flare law stability. A less than critically damped flare law will cause second or third overshoots of the nominal flare path. In such a case, one could expect an initial flare law overshoot after the flare law is first engaged and the aircraft initiates a response. Later in the flare, the aircraft might experience a second overshoot above the profile due to overcorrection from subcritical damping. However, since aircraft maneuvers are generally very limited during flare for safety reasons, most flare laws are heavily damped. This implies that in the absence of disturbances, the aircraft will not experience a second overshoot. As discussed earlier, headwind or tailwind cases might initially overshoot the computed profile to a greater or lesser extent than the no-wind case. Therefore, flare law damping considerations are important when wind cases are compared to no-wind cases. Even though two flare laws are heavily damped, the lesser damped law may contribute to a second overshoot of the no-wind profile while the more heavily damped law might not allow a second overshoot.

The overall dominant trends for the constant headwind case can be summarized by four observations. First, lower initial vertical speed allows less flare law overshoot at flare initiation and softer pitch commands later in flare. Second, lower groundspeed reduces the amount of range covered per unit time, which is the only independent variable in the flare law equation. Thirdly, a longer time to flare causes more of a throttle retard, reducing control effectiveness to flare commands at the end of flare. Finally, flare law damping will determine the possibility of mild oscillations in the flare path.

The analysis of tailwind landings can be done by analogy to the previously discussed headwind/no-wind comparison. The tailwind flare compared to a no-wind flare looks like a no-wind flare compared to a headwind flare. That is, a tailwind causes even more initial flare law overshoot, greater pitch commands, higher groundspeeds and a shorter time of flight.

From the description of the effects of constant winds, one could comment that it appears that wind changes the stability of the tracking task. In effect, this is exactly what happens. With non-adaptive gains in the autopilot, a higher groundspeed caused by a tailwind destabilizes the aircraft on its approach along a glide path fixed in space. Similarly, a headwind increases the stability of the aircraft during glideslope tracking.

Figures 6 and 7 show various magnitudes of headwinds and tailwinds, which are a family of curves.

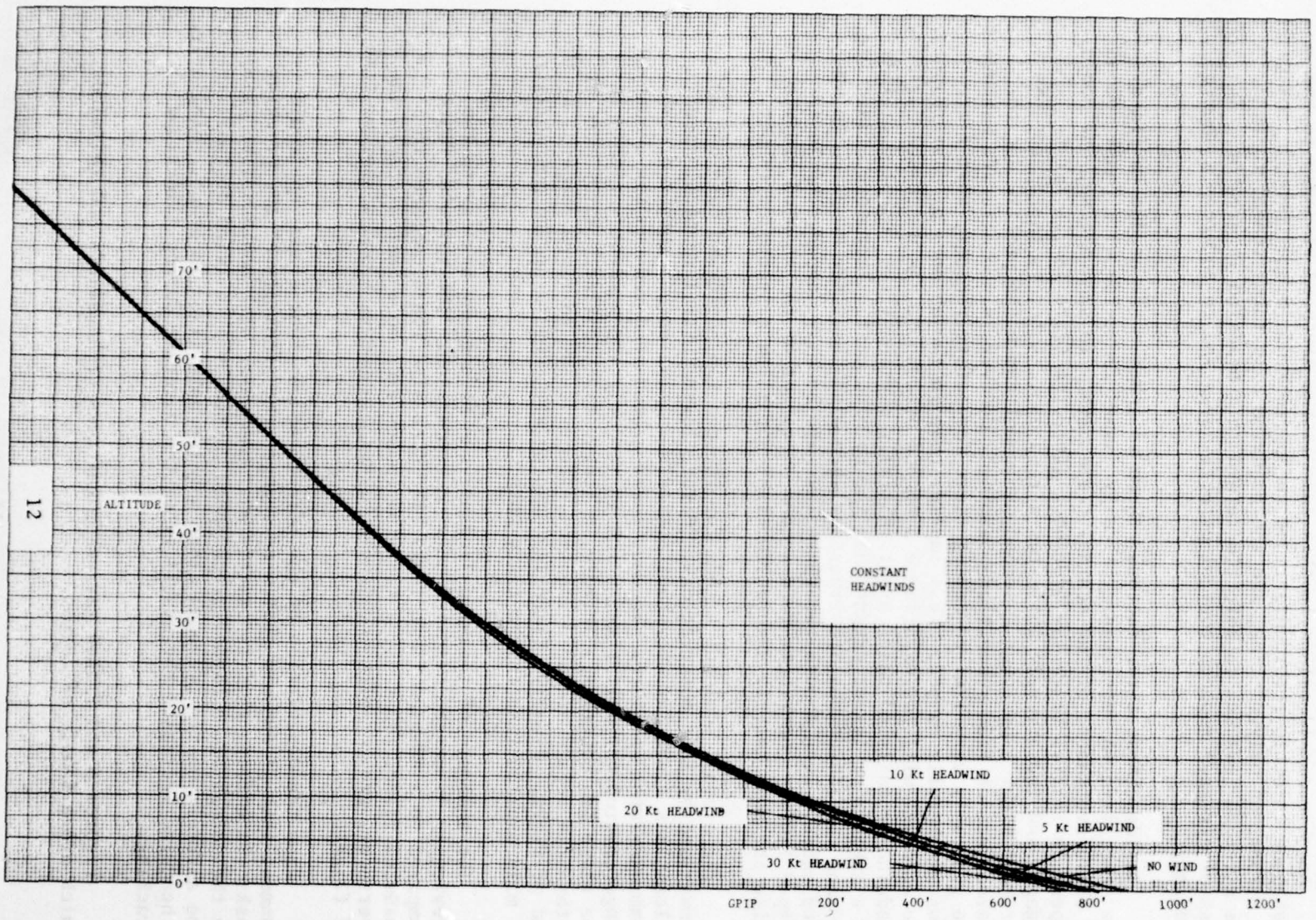

FIGURE 6. Flare Paths in Various Headwinds

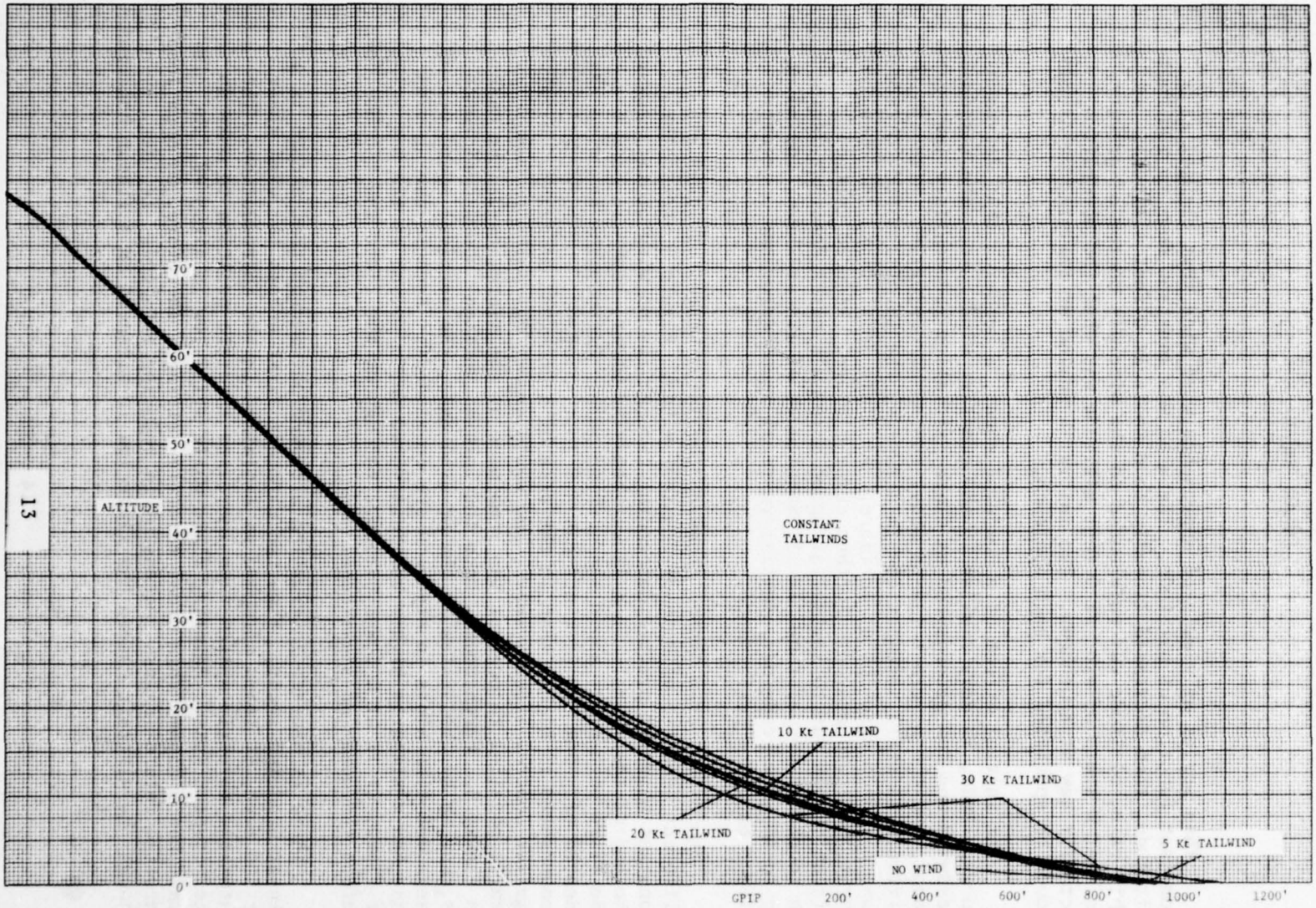

FIGURE 7. Flare Paths in Various Tailwinds

SECTION IV

LINEAR SHEAR

This series of simulated approaches used wind that changed as a constant function of altitude. The wind was constant down to 500 feet altitude, then decreased linearly to 0 knots at 0 feet altitude. In this case, altitude was referenced to the aircraft center of gravity, so that 0 knots of wind at 0 feet altitude was what the aircraft actually saw at touchdown. The initial headwind or tailwind magnitude could be specified for each approach.

The initial effect of a headwind shear, a headwind that decreases in magnitude, is very similar to the constant wind case. The residual headwind and low groundspeed at flare initiation reduce flare law overshoot, and the aircraft flares above the no-wind profile. Although the aircraft is still somewhat low in airspeed, the throttles had corrected some airspeed error prior to flare. At flare initiation, the open loop throttle retard prevents further error closure. Reduced control effectiveness due to initial airspeed error was not a dominant factor in touchdown dispersion. In all magnitudes of linear shear, including up to 40 knot headwinds, initial vertical speed error had a greater effect on flare performance.

The effect of a linear shear on the later stages of flare are different than the effects of constant winds. Figure 3 showed the constant headwind profile descending through the no-wind profile toward the end of the flare. In a linear headwind shear, shown in Figure 8, the flare path stays above the no-wind path. Because the headwind has sheared off, but the aircraft has not lost airspeed, the aircraft's groundspeed is higher than in the case of a constant headwind. With similar control effectiveness, one would expect the paths to remain nearly parallel throughout the remainder of the flare, as is the case in Figure 8. Furthermore, once the initial vertical speed difference is made up by the system in the no-wind case, the vertical speed versus range and time plots in Figure 9 are coincident. Because the no-wind case had a slightly higher vertical speed for a period at the beginning of flare, it is at a lower altitude throughout the flare and touches down before the headwind shear case.

There is another interesting airspeed phenomenon that occurs in a linear headwind shear. When the aircraft first enters the wind shear at 500 feet, it loses airspeed as explained in the introduction. The automatic throttle system then increases throttle position to make up the airspeed loss. Entering flare while still low in airspeed, the aircraft has a higher than usual throttle setting. Therefore, an open loop throttle retard is less successful in reducing airspeed. In fact, even though the aircraft enters the flare low in airspeed in a linear headwind

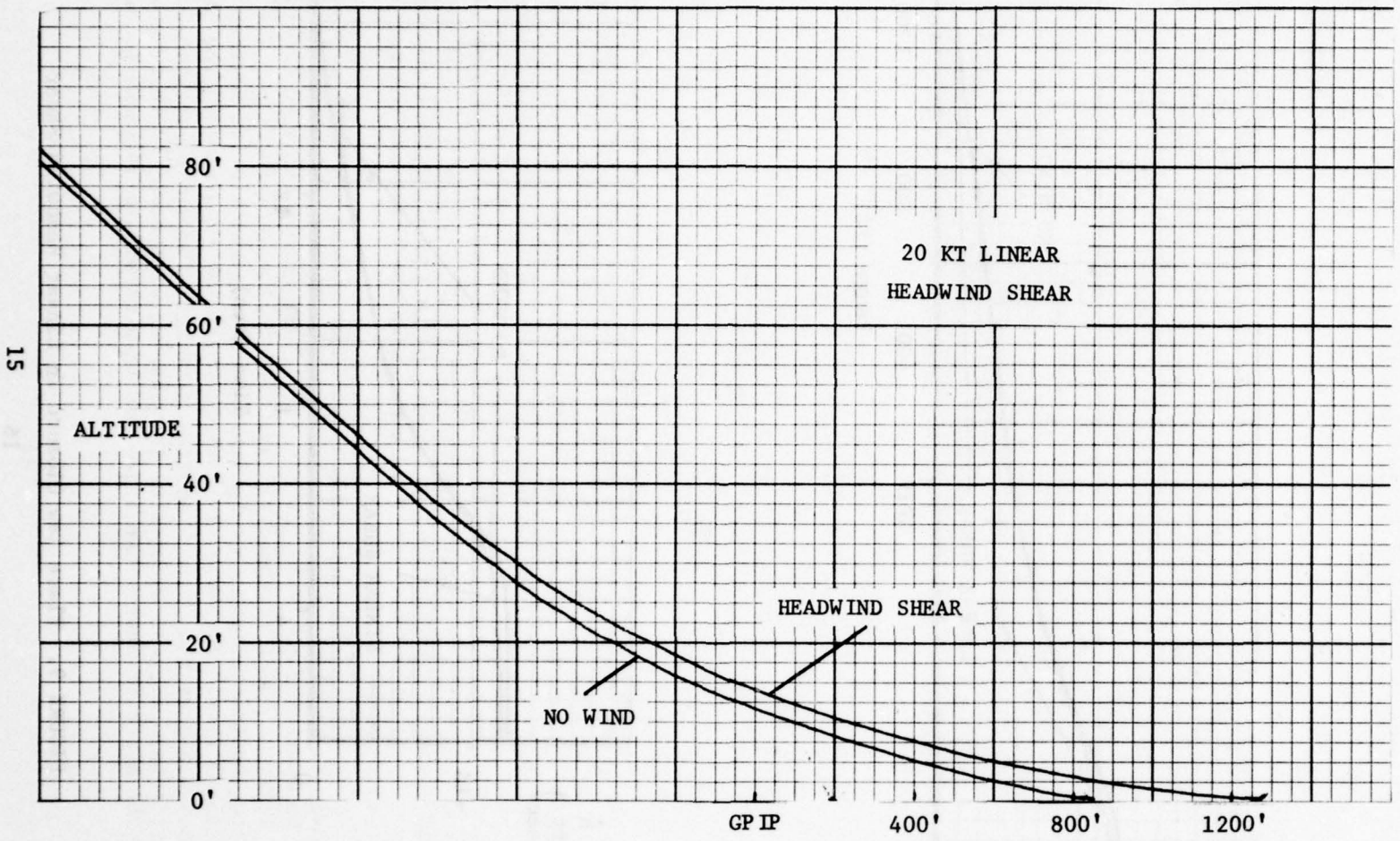

FIGURE 8. Flare in a 20KT Linear Headwind Shear

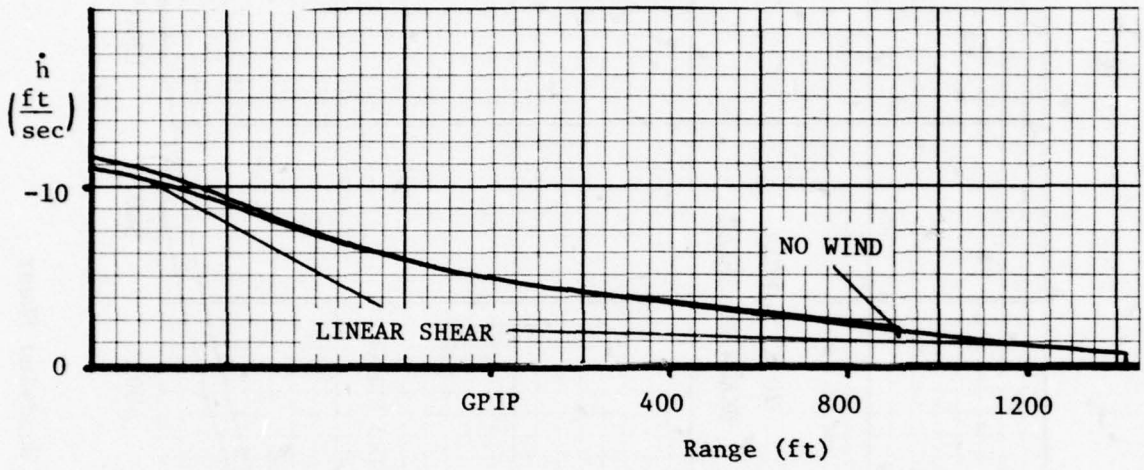

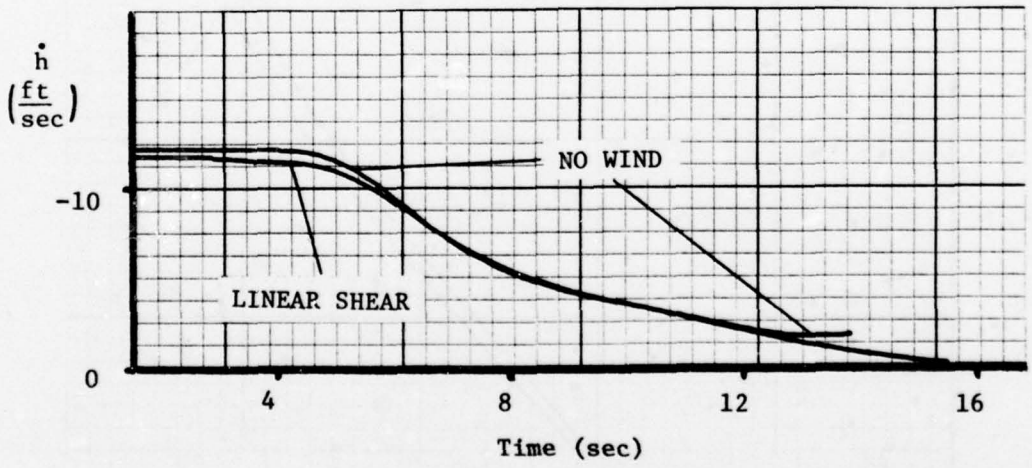

FIGURE 9. Flare Law Closure In Linear Headwind Shear

shear, the rate of airspeed loss during flare is small enough that the airspeed near the end of flare is the same or higher than the airspeed in no-wind. When this airspeed excess is combined with the higher flare path in the linear headwind shear case, the result re-enforces a longer touchdown point.

Predictably, a linear tailwind shear has the opposite effect on longitudinal touchdown point. As it descends, the aircraft is decelerated by the decreasing tailwind component. A higher sink rate at flare initiation due to the remaining tailwind and high airspeed contribute to a large vertical speed overshoot of the computed schedule. Throttles are already somewhat retarded in an attempt to regain proper airspeed, and the open loop retard at flare creates such a thrust deficient condition that airspeed is lost very quickly. The ultimate result is a short and hard landing. Various magnitudes of linear shears are illustrated in Figures 10 and 11.

Once again, the effects of linear shears are dependent on the flare law, aircraft, and throttle system. One would expect intuitively that a decreasing headwind causes shortened flare in an automatic landing, and this has been the case in some previous studies in the literature (Ref 2). However, the reason for a short flare in previous studies is a loss in airspeed. As discussed earlier, there was a loss in airspeed for this system, but other effects were dominant. The analysis of logarithmic shear later will illuminate some interesting contrasts with the linear shear.

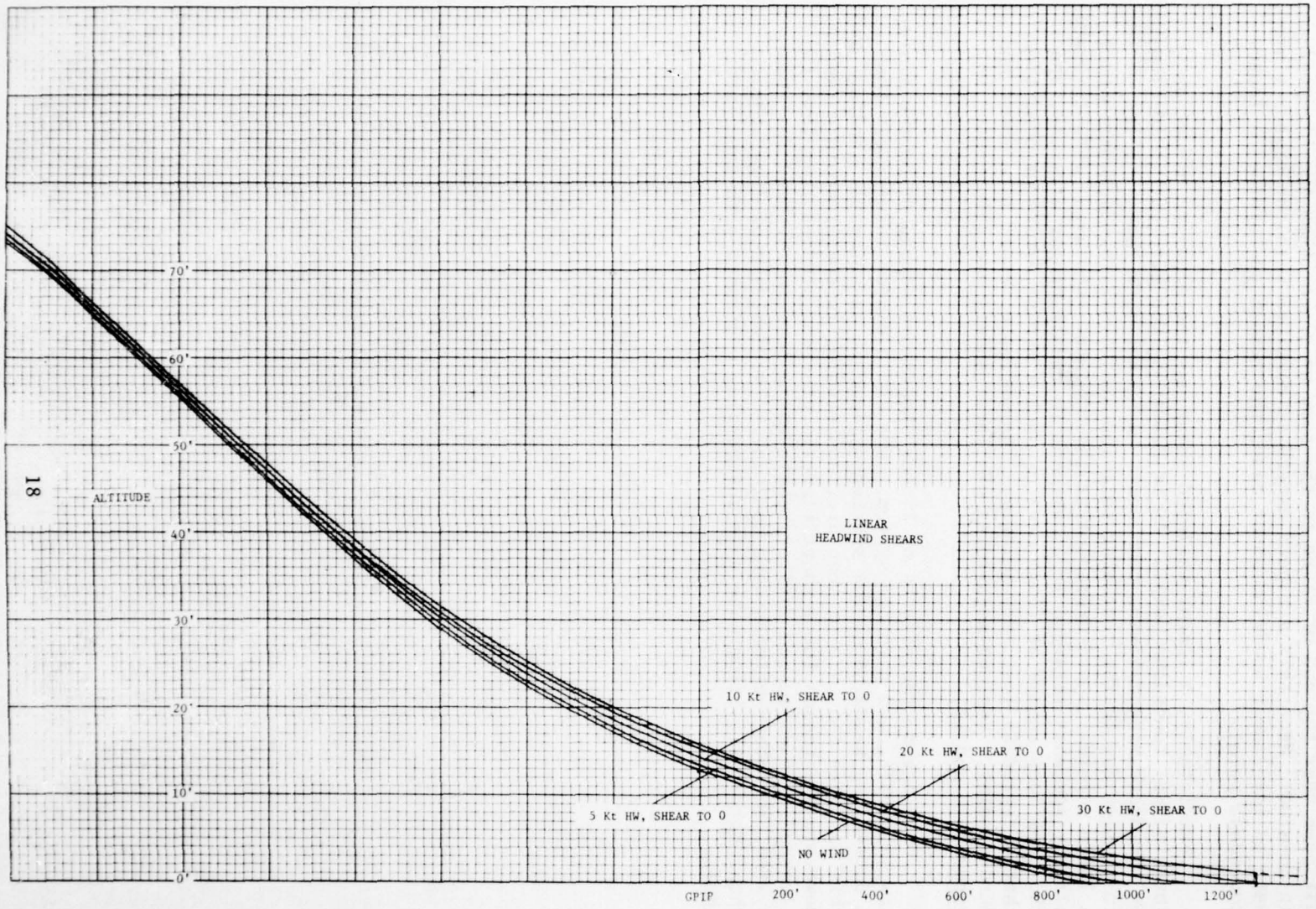

FIGURE 10. Flare Paths in Various Linear Headwind Shears

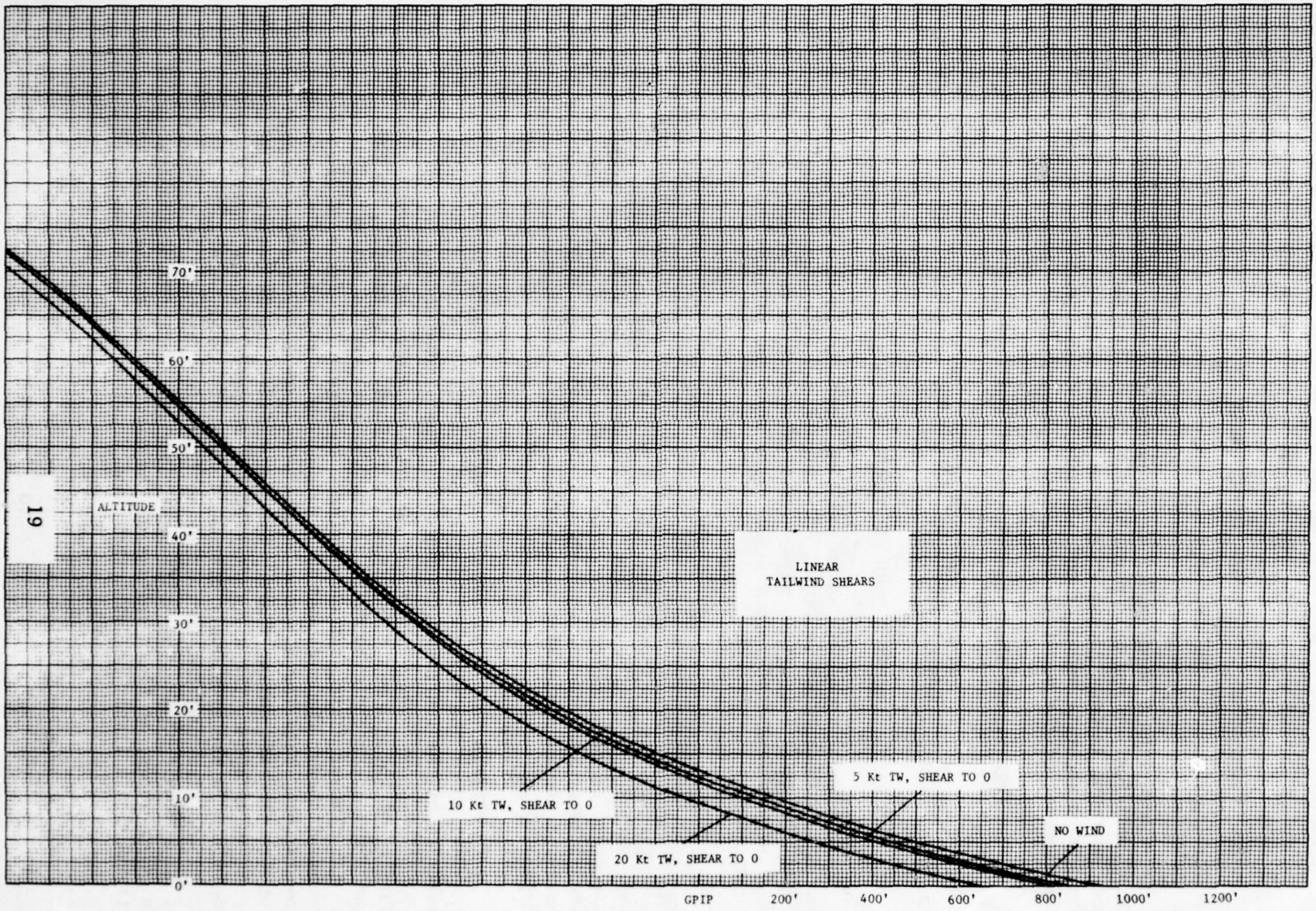

FIGURE 11. Flare Paths in Various Linear Tailwind Shears

SECTION V

LOGARITHMIC SHEAR

A logarithmic shear model was used for the next shear condition. The justification for this particular mathematical description of shear can be found in many recent references and is currently considered to be a more accurate model of actual measured shears (Ref 3). The development of the model is explained in Appendix A.

The logarithmic shear equation is of the form:

$$\text{Wind Velocity} = V_w = C \ln \frac{h}{h_o}$$

where h = wheel height

This shear model has an interesting property in that it has an infinite number of derivatives. The significance for an automatic flare system is that it is theoretically impossible to build a closed loop system which can zero a flare error when the disturbance is logarithmic.

The performance of the aircraft in simulation is as poor as the mathematical prediction above. Range and sink rate dispersions were much greater due to logarithmic shears than with linear shears. An even more surprising result was that dispersions were in the opposite direction of the linear shear cases. Compared with a no-wind case, logarithmic headwind shears yielded a shorter flare, while linear headwind shears produced a longer flare. This is illustrated in Figure 12.

To explain this apparent contradiction in results requires an examination of the airspeed history of the flare in addition to an analysis of the inertial states as done for linear shear. A logarithmic increase or decrease in the wind speed far exceeded the ability of the automatic throttles to respond. For example, in the case of a logarithmic headwind shear, the airspeed is not only low at the time of flare, but decreasing. In Figure 13, for a 20 knot headwind shear, the airspeed is 3 ft/sec low at the time of flare initiation. This low airspeed slightly reduces control effectiveness for the aircraft during flare. Since the flare law is designed for a specific airspeed, the aircraft will not respond to flare commands as rapidly. In the previously discussed case of linear shear, the airspeed was also low, but increasing at flare initiation. In the case of logarithmic shear, the initial airspeed is lower and decreasing. In other words, at flare initiation the aircraft is accelerating in airspeed in a linear headwind shear and decelerating in airspeed in a

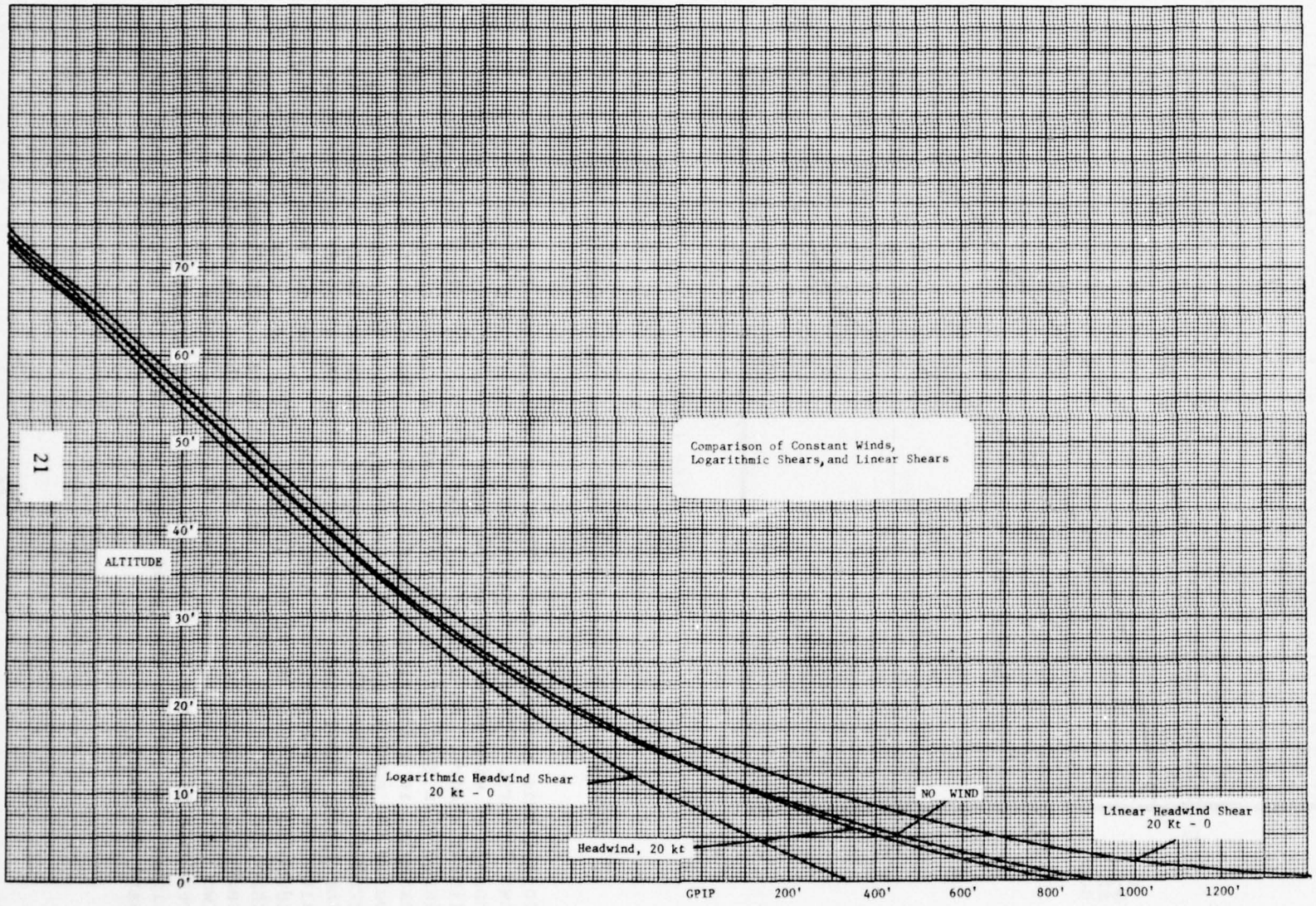

FIGURE 12. Comparison of Flare Paths in 20 Knot Logarithmic and Linear Headwind Shears

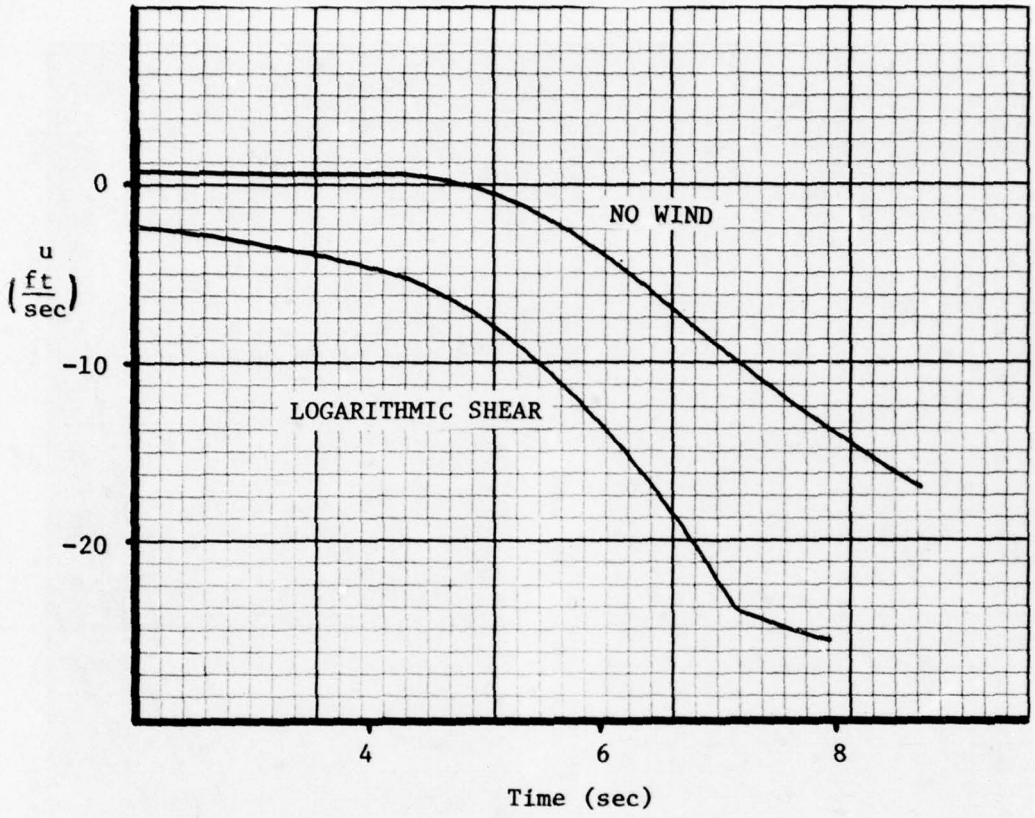

FIGURE 13. Airspeed In A 20KT Logarithmic Headwind Shear

logarithmic headwind shear. This can be explained by a combination of two factors. First, a logarithmic wind shear has a higher rate of change of wind magnitude at the lower altitudes than with comparable linear shears. An aircraft at flare altitude is likely to experience large wind gradients and therefore large airspeed changes. For example, in a logarithmic headwind shear, the aircraft is significantly below the nominal airspeed. Secondly, because the onset of shear is gradual, the throttles do not respond as much initially as they do in the linear shear case. Consequently, when the aircraft reaches flare altitude in a logarithmic headwind shear, it does not have the greatly advanced throttles as in the linear headwind shear case. Therefore, throttle freeze and retard at this point have a significant effect on reducing airspeed even further. Figure 14 shows the results of these two factors. The aircraft starts flare at a rather low sink rate, but response is so poor that the sink rate is not arrested well. With the higher sink rate in the later stages of flare, the aircraft lands both hard and short.

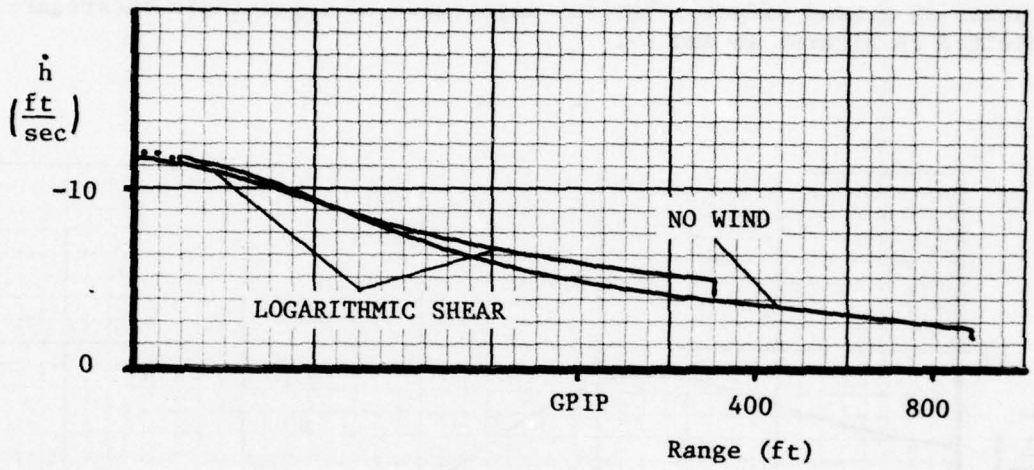

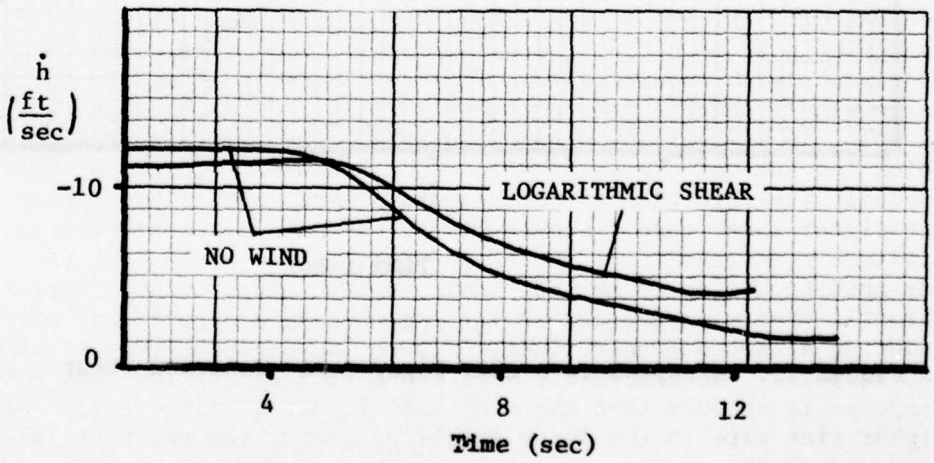

FIGURE 14. Flare Law Closure In Logarithmic Headwind Shear

In a logarithmic tailwind shear, the aircraft is high in airspeed at flare initiation. The throttle retard is not effective in correcting the situation, since it takes about 5 seconds after flare initiation just to return the airspeed to the initial flare value, as shown in Figure 15. With this excess airspeed, the aircraft easily closes out the flare law error, and in fact, overshoots the error due to excessive control response. This causes the aircraft to depart above the no-wind profile, and extends the flare to a very soft touchdown as the aircraft floats in ground effect. Various magnitudes of logarithmic shears are plotted in Figures 16 and 17.

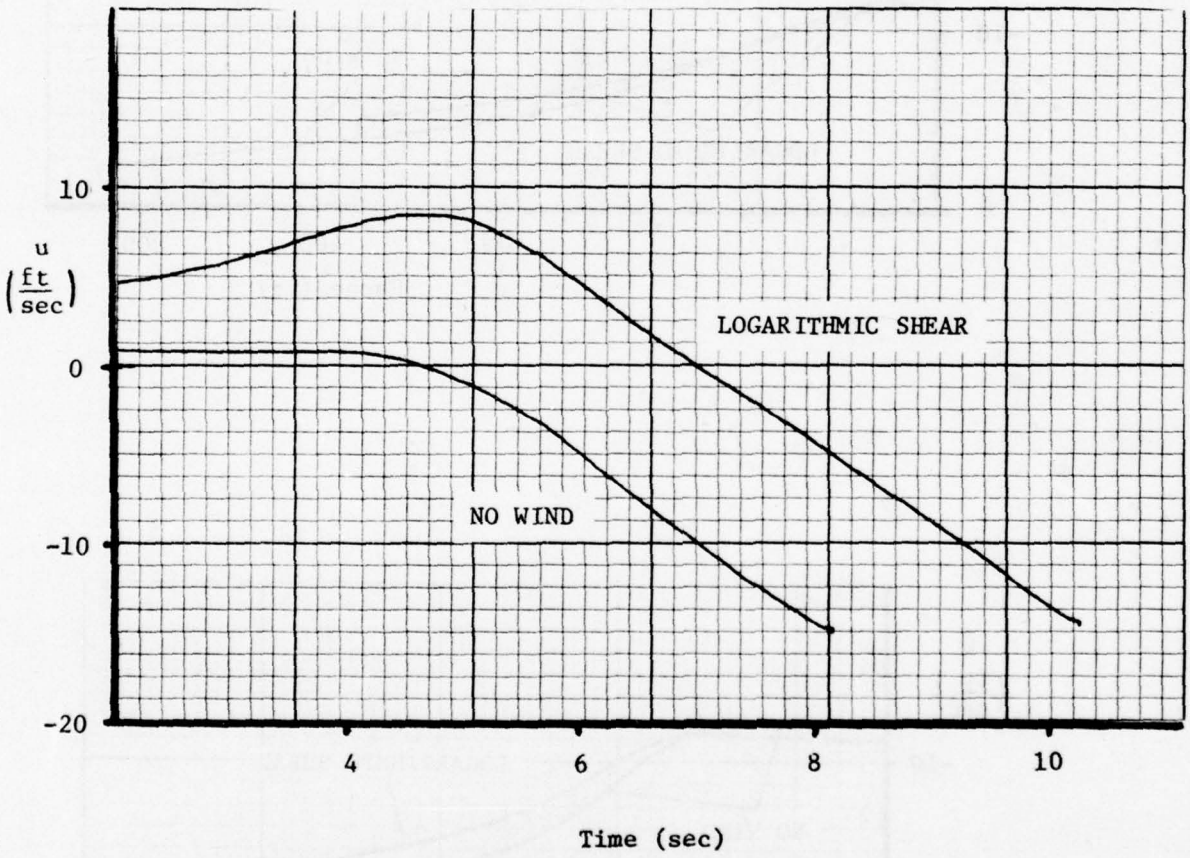

FIGURE 15. Airspeed in a 20KT Logarithmic Tailwind Shear

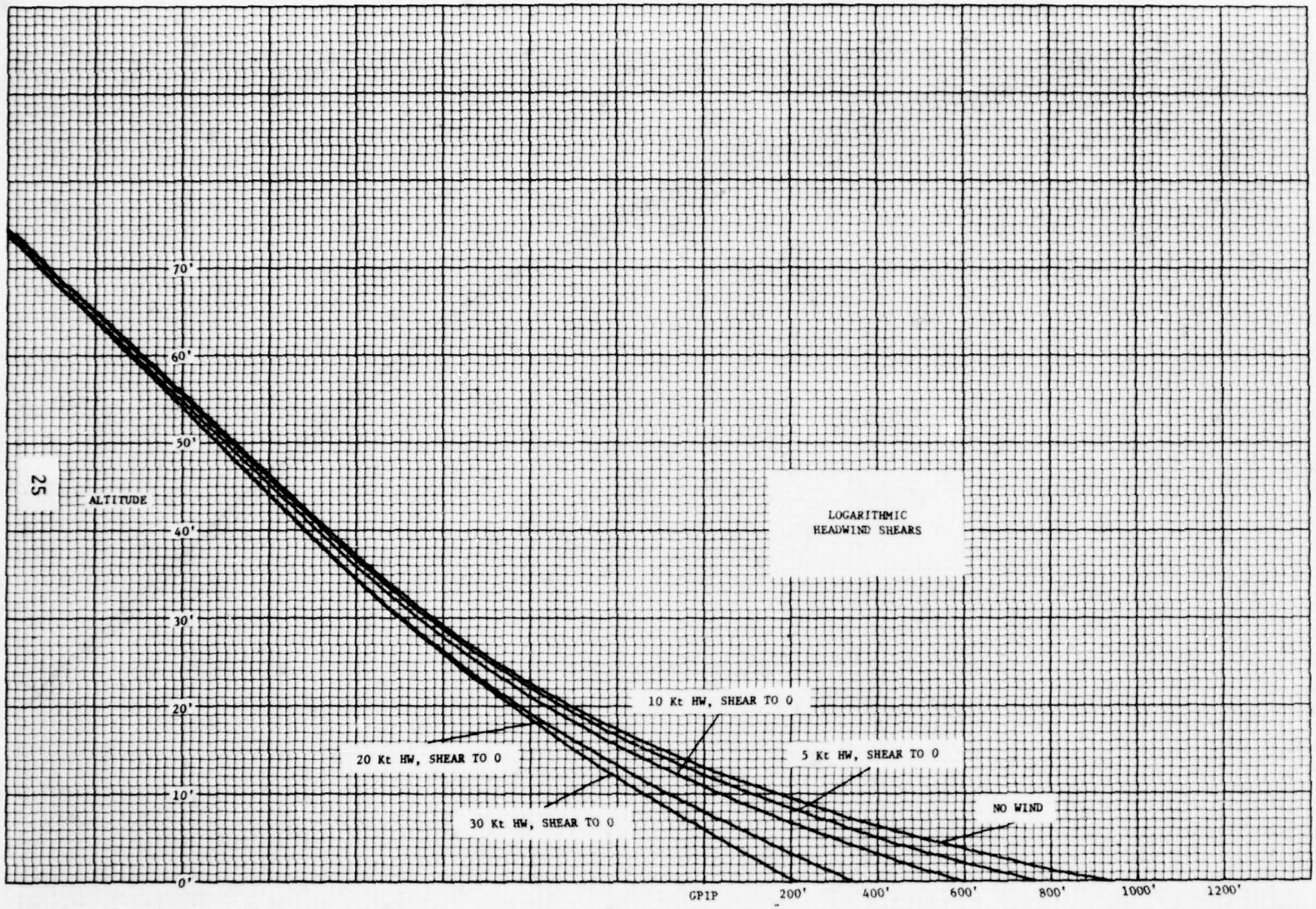

FIGURE 16. Flare Paths in Various Logarithmic Headwind Shears

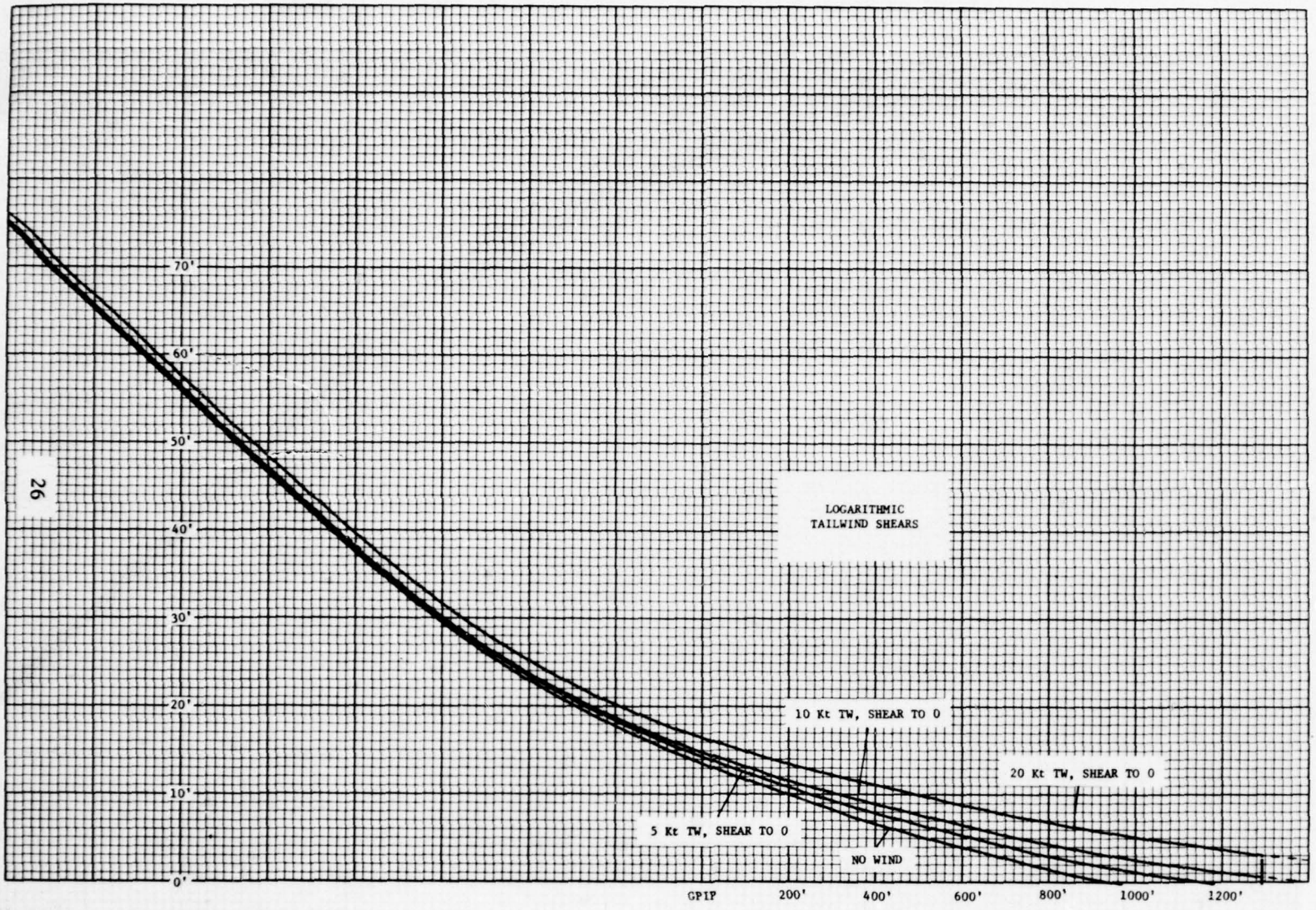

FIGURE 17. Flare Paths in Various Logarithmic Tailwind Shears

It is interesting to note that as the shear initiation altitude is chosen lower, a linear shear becomes a piece-wise linear approximation to a logarithmic shear in the flare regime, and results are similar to the logarithmic shear case. Mathematically, this can be explained by the presence of the discontinuity between constant wind and the linear shear. The aircraft is responding to a highly non-linear input, which results in a transient at the time of flare. Figure 18 illustrates this comparison.

One further significant relationship exists between a certain class of logarithmic shears. For a shear of a given magnitude, the longitudinal dispersion is not directly related to the final wind value. That is, a shear from 40 knots to 20 knots does not produce a worse dispersion than 20 knots to zero. In fact, as shown in Figure 19, these parameters are somewhat inversely related. The longitudinal dispersion is actually reduced slightly in the higher wind condition. The reason for this is that the higher or lower groundspeed, caused by the remaining wind and inertia, opposes the effect of the airspeed gain or loss due to the shear. For example, in a 40 knot to 20 knot headwind shear, the aircraft still has a significant headwind during flare. This reduces flare law overshoot and increases the aircraft's ability to fly the computed flare law path, as in the constant headwind case. Therefore, low airspeed caused by the shear is less of a problem. A 20 knot to 10 knot shear has the same airspeed problem due to the same magnitude shear, but does not have the advantage of a higher overall headwind.

This relationship is significant for logarithmic shears. In aircraft operations, high ground winds are often considered indications of an increased probability of shear. However, for some autoland systems, it is possible that a smaller shear occurring with a lower ground wind can more greatly endanger the landing.

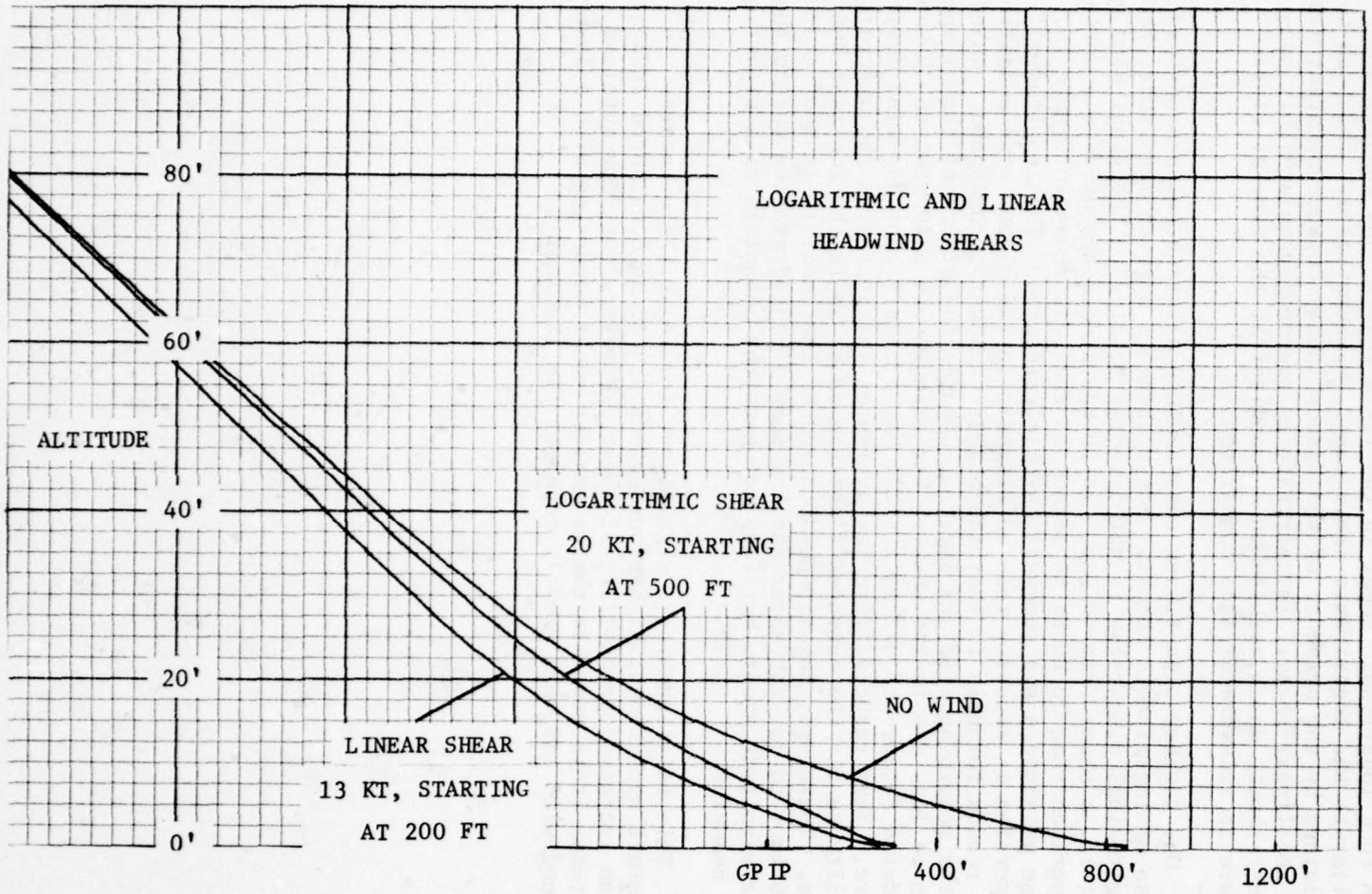

FIGURE 18. Low Altitude Linear Shear

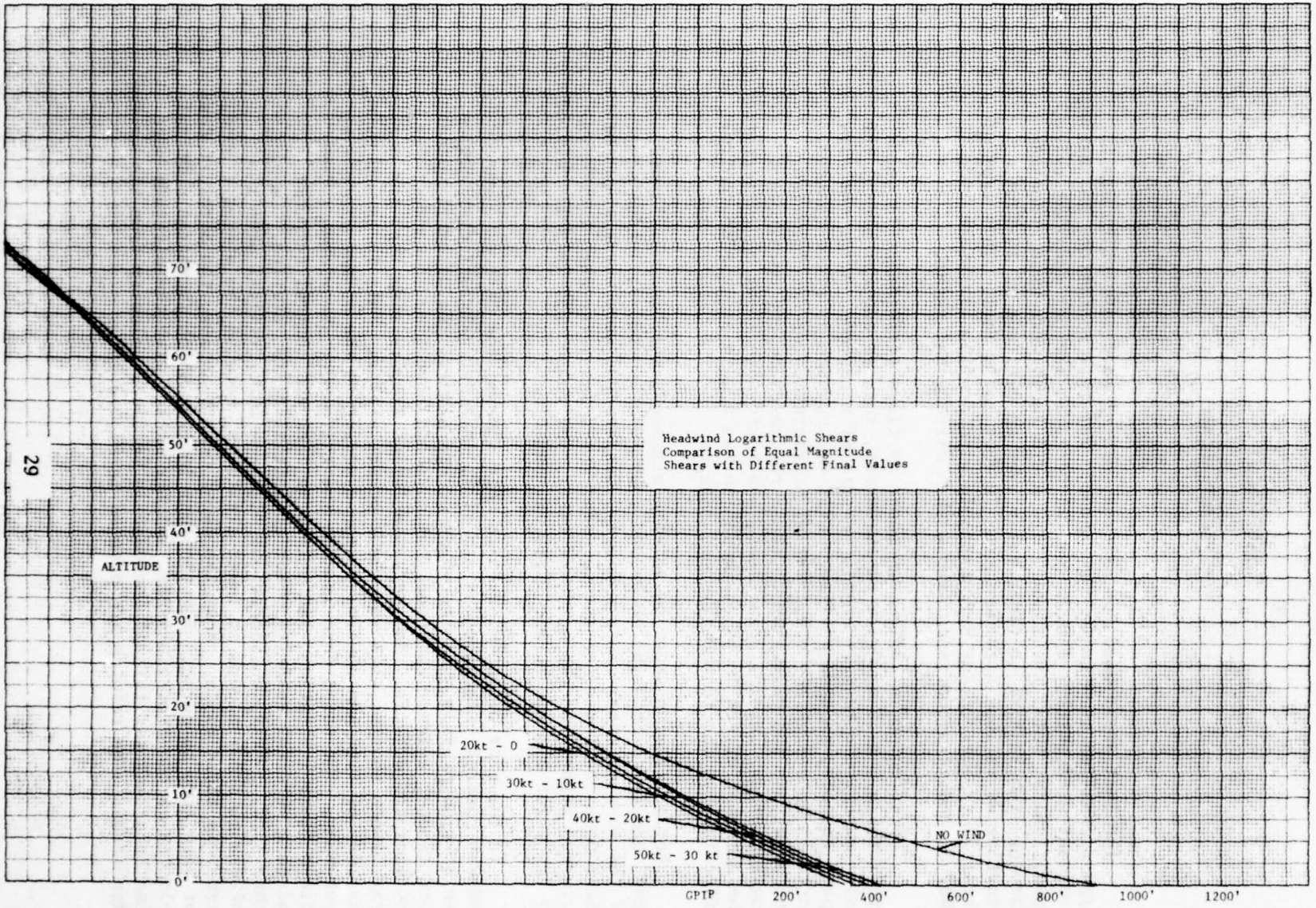

FIGURE 19. Shear Effects on Flare in Various Levels of Winds

SECTION VI

KNIFE-EDGE SHEAR

The last shear used for aircraft disturbance simulation was a type classified as a knife-edge shear. For this condition, an initial constant wind quickly shears several knots to another constant value. Specifically, total shears of 2 1/2 and 5 knots were used, smoothly varying from initial to final value over an altitude of 10 feet, starting at various altitudes from 70 feet to 20 feet. This type of shear is typical of the very unstable wind profile classification (Ref 3) and is often associated with a directional shear.

The effect of a knife-edge shear on flare performance is quite predictable. With no prior disturbances, such as another shear, the only immediate effect is a gain or loss of airspeed. After the airspeed changes, secondary effects will occur, such as pitch changes, vertical acceleration, and inertial acceleration or deceleration. The magnitude and direction of these responses depend on aircraft configuration, initial conditions, and knife-edge shear characteristics. The dominant effect in this simulation was a gain or loss in control effectiveness due to the airspeed change.

For a tailwind shear or gain in airspeed, the aircraft landed long; and for a headwind shear and loss in airspeed, it landed short of the no-wind case. Interestingly, dispersions were worse when the shear occurred lower for the tailwind case, and worse when the shear occurred higher for the headwind case. The reason for this is related to the error closure in the flare law equation.

In the case of headwind knife-edge shears, the loss of airspeed reduces control effectiveness and lift, thus the aircraft drops below the no-wind profile. If the shear occurs higher, the aircraft spends more time at a lower airspeed, but also has more time to correct for the airspeed deficit. However, simulation results show that the aircraft lands shorter when the shear occurs higher. This is caused by the loss of lift and control response adding to the normal flare law overshoot. The worst case is when the knife-edge shear occurs just before flare initiation, and a loss in lift and control response increase vertical velocity prior to initial flare rotation. On the other hand, safety considerations might be more critical when the knife-edge shear occurs at lower altitudes, because the aircraft lands harder in these cases. When the shear occurs so low, the aircraft does not have time to correct for the loss in lift which increases vertical velocity as the aircraft lands. Higher shears give the aircraft more time to arrest the initial increase in vertical velocity from the knife-edge shear. The results are plotted in Figure 20.

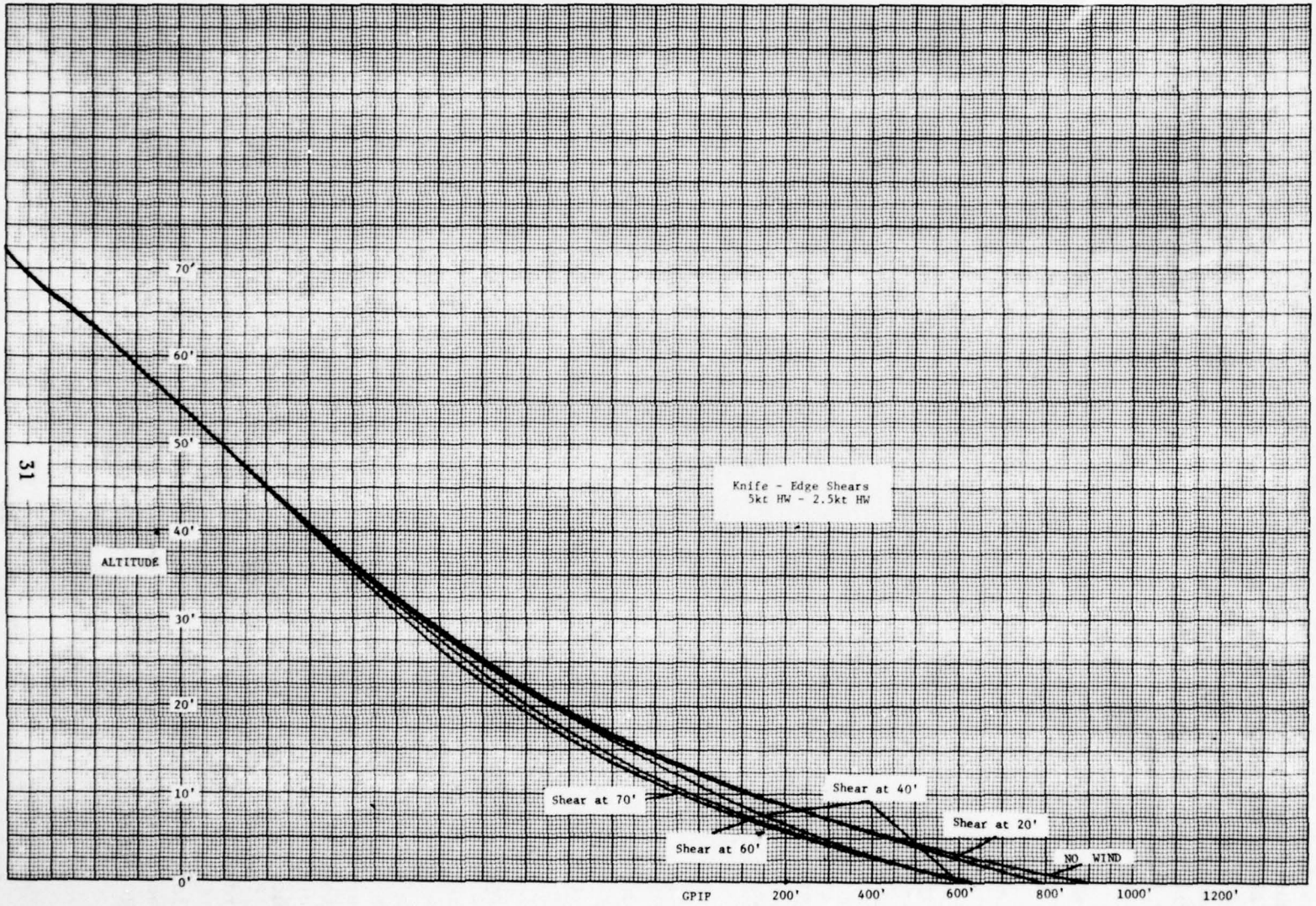

FIGURE 20. Flare Paths in Headwind Knife-Edge Shears

For tailwind shears, the gain in airspeed aids the error closure. At a high altitude, the initial flare vertical velocity error is reduced and the aircraft more closely holds the nominal profile, which is above the no-wind case. But, as the shear occurs lower, the error is already minimized and the aircraft overshoots the nominal profile, illustrated in Figure 21. The overshoot, coupled with nose-down control limitations and ground effect, results in a longer touchdown point than the no-wind case.

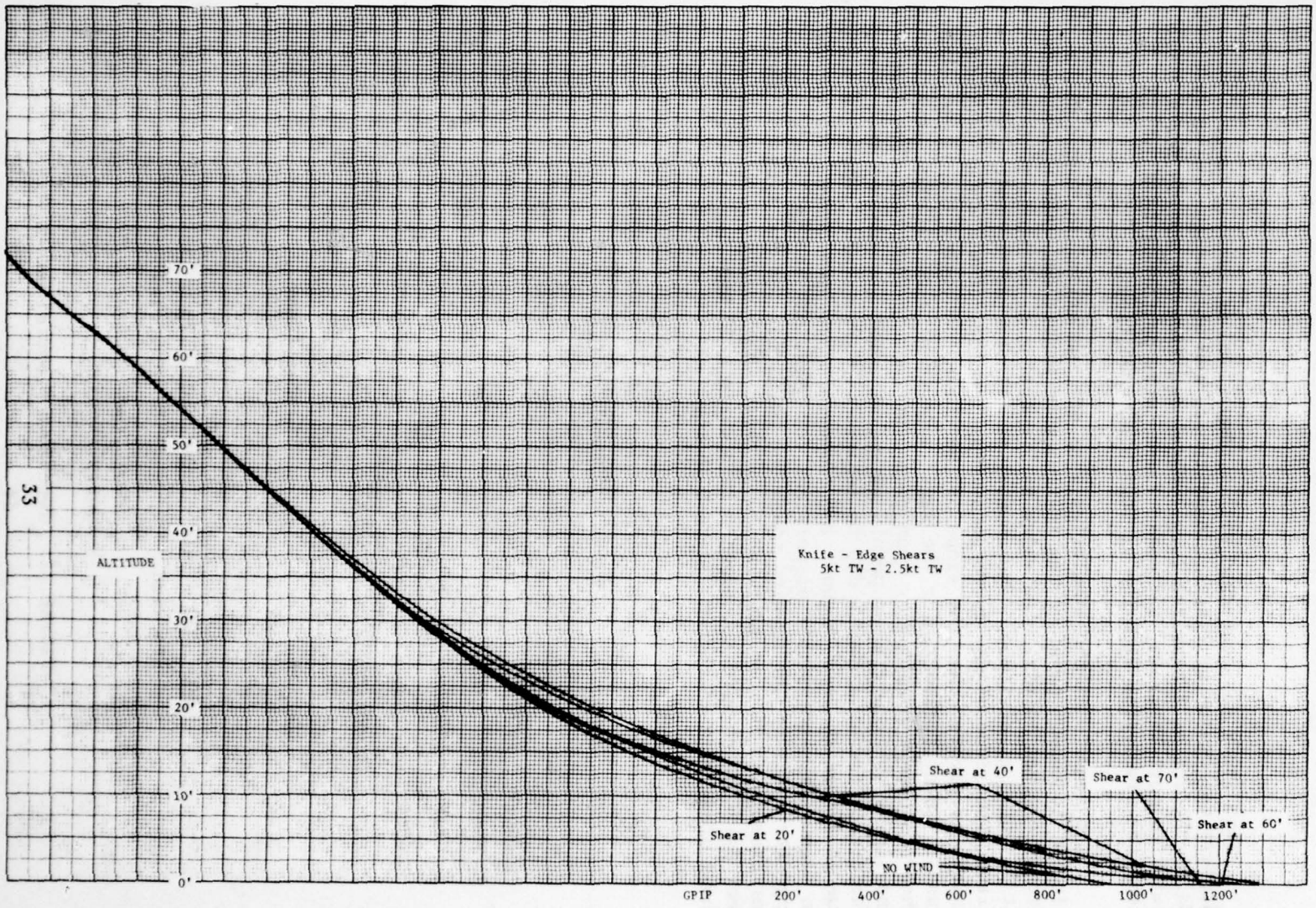

FIGURE 21. Flare Paths in Tailwind Knife-Edged Shears

SECTION VII

DISCUSSION OF RESULTS

This study was concerned with a comparison of landing range dispersions caused by linear, logarithmic, and knife-edge wind shears. Using the set of linearized longitudinal equations of motion for a large jet transport aircraft, automatic flares were performed in a hybrid computer simulation with the various wind conditions.

The results of the simulation runs are summarized in Figure 22, a plot of touchdown point versus initial wind magnitude. All shears were from the given initial wind value at 500 feet c.g. altitude to 0 knots at 0 feet c.g. altitude. The comparison illustrates two main points. First, the slope of the curve connecting the logarithmic shear touchdown points is greater than the slope of the curve connecting the linear shear cases. Quantitatively, for the same range of wind conditions, logarithmic shear touchdown points vary from about 200 feet to 2100 feet from the GPIP, and linear shear touchdown points vary from about 700 feet to 1600 feet. Therefore, the dispersions due to logarithmic shears are greater than those due to linear shears. Second, the slopes of these two curves are opposite in sign. This means that dispersions for headwinds and tailwinds are on opposite sides of the no-wind touchdown point for the two types of shear. For example, a 20 knot tailwind logarithmic shear causes a landing 1050 feet past the no-wind touchdown point, while a 20 knot tailwind linear shear produced a touchdown 350 feet short.

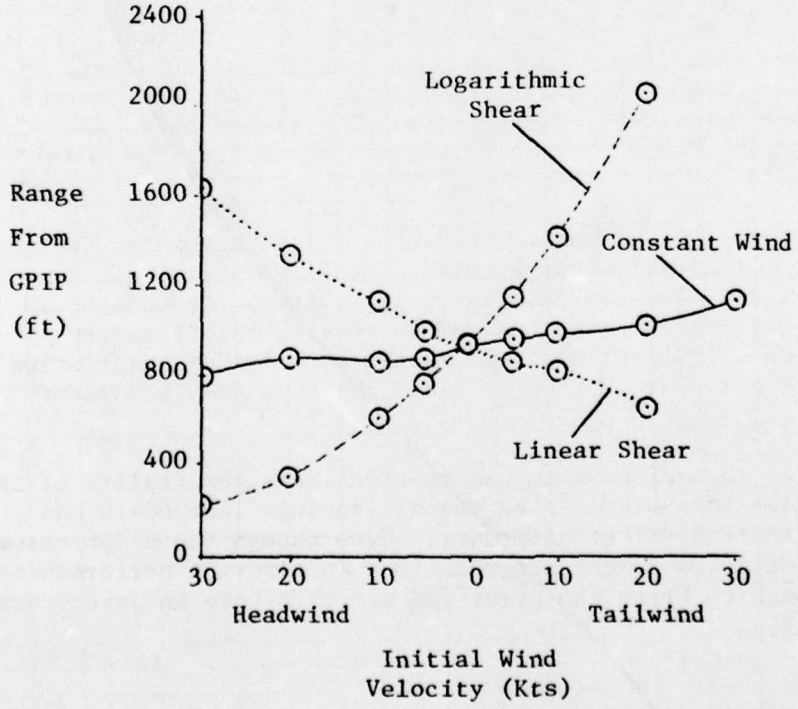

FIGURE 22. Touchdown Dispersions

As some indication of the implications of this study on manual approaches, an actual airline accident profile was simulated. On 17 December 1973, Iberia Flight 993, a DC-10, crashed short of Runway 33L at Boston's Logan Airport. The National Transportation Safety Board cited excessive wind shear as a primary contributory factor in the crash. Wind magnitudes and directions were available from the flight recorder at 100 feet intervals. These were converted to magnitudes in the direction of Runway 33 and used in a simulated approach for the aircraft and flight control system in this study. Figure 23 shows the actual approach path and the wind profile. The result was a landing 84 feet short of the GPIP with a touchdown sink rate of -5.4 ft/sec. A typical zero-wind landing lands 920 feet past the GPIP at a vertical speed of about -2.5 ft/sec.

An analysis of this profile can be made based on the work in the previous sections. The wind starts out as a 32 knot tailwind, and shears to a 15 knot tailwind by 400. The shear rate increases then to about 8.5 kt/100 feet to 100 feet altitude where the wind is a 7 knot headwind. A tailwind shear, as shown earlier, increases airspeed. The aircraft departed above the glide slope due to insufficient throttle response to this airspeed increase. Over the last 100 feet, the wind remains almost constant. Since the aircraft has been responding to essentially a linear shear, the autothrottle has been reducing throttle position to decelerate the aircraft to the correct airspeed. However, when the wind remains constant, the airspeed falls off as the aircraft continues to decelerate in its thrust deficient configuration. The problem is further complicated by throttle retard during flare. Since ground speed has been high due to the tailwind component, the aircraft has little time to increase pitch. In the simulated approach, the aircraft was 2 knots high in airspeed and decelerating at 100 feet. Sink rate was .8 ft/sec high. By flare initiation, airspeed was correct, but decreasing very rapidly. Sink rate was 1.1 ft/sec high, and increasing. The touchdown parameters, described earlier, included a short landing with a sink rate of -5.4 ft/sec.

This shear profile was one of the worst for an automatic landing. First, the strong tailwind shear elicits pitch down and throttle reduction maneuvers. Then, a constant wind reverses the command in the autopilot, calling for pitch up and increasing throttle. By occurring at such a low altitude, the result is a lot of unsatisfied commands with errors that show up as excessive touchdown parameter errors.

The point of this discussion was to illustrate the reality of the wind shear problem for automatic or manual landings (the DC-10 was autopilot coupled to 100 feet altitude). Even though the pilot assumed control at the decision height, degradations in aircraft performance were subtle enough to bring the pilot and aircraft into an unrecoverable situation (Ref 4).

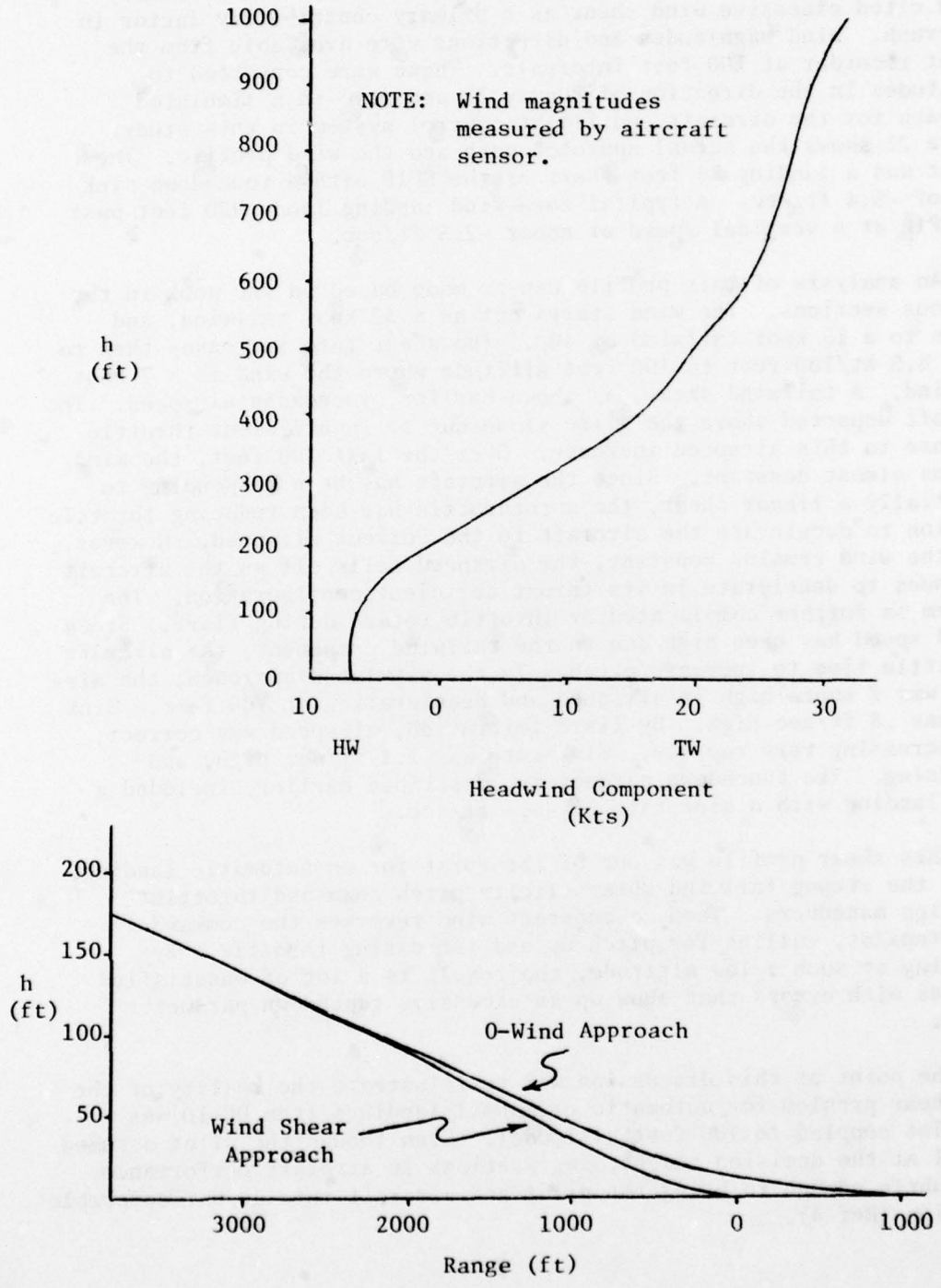

FIGURE 23. Wind Profile and Simulated Flight Path

SECTION VIII

CONCLUSIONS AND RECOMMENDATIONS

This study has yielded support for three conclusions on the effects of wind shear on automatic landing. The conclusions, of course, are based on the particular aircraft and automatic flight control system used. The conclusions are:

1. Logarithmic wind shear causes landing dispersions to the opposite side of the no-wind touchdown point from linear wind shear.

2. For the same magnitude and initiation altitude of wind shear, landing dispersions due to logarithmic wind shear are significantly greater (often two or three times) than dispersions due to linear wind shear.

3. Dispersions in touchdown point and vertical speed at touchdown may be great enough to affect the safety of the landing.

The implications of these findings appear to be significant for automatic flight control system design. Until very recently, most criteria for system certification have been based on linear shear profiles. For an aircraft and flight control system of the category used for this study, this could yield results that are not only conservative in magnitude, but erroneous in overall trend. Certifying an aircraft flight control system based on a computer analysis of linear shears could cause some surprises when the aircraft later encounters logarithmic shears in actual operations.

The third conclusion states that shear can cause very serious problems in an automatic landing regardless of the type of shear. In a 30 knot logarithmic headwind shear, for instance, the landing was only 219 feet from the GPIP and the touchdown sink rate was -6.2 ft/sec, which is approaching safety limits for a large aircraft. Headwind knife-edge shears of only 5 kts at 20 feet c.g. altitude caused a similar result. These shears, when compared with actual wind reports (Ref 1), do not seem to be unrealistic, suggesting that more design work is needed in the area of automatic flight control to reduce the effects of these disturbances.

A word of caution is appropriate in describing the effects of wind shear on landing. As repeated several times throughout this report, many of the results of this study were dependent on the configuration of the aircraft and flight control system. Any generalization of these results to other aircraft must be done carefully. Even more important,

generalization of these results to manually flown approaches must be done with care. For example, common problems in manual approaches in wind shear are undershooting the runway in tailwind shears and overshooting the runway in headwind shears. This is contradictory to the results found in this study for logarithmic shears. However, careful examination of these manual landings shows that the landing dispersion is due to the pilot's overcorrection of the shear effects and not due to the shear alone. A headwind shear, for instance, causes a loss of airspeed and lift. The reaction of the pilot is to increase power settings, and if glideslope deviations are large enough at low altitudes, he might increase pitch attitude to return to the glideslope. Since his correction is usually not "critically damped", in a control sense, especially if he is concerned about the safety of the approach, he is essentially in an "overshoot" condition at the time of landing. Thus, he finds himself high and fast at the end of flare. Of course, a shear of large enough magnitude might prevent the pilot from regaining the correct airspeed or glideslope at all, thus yielding the same result as with the autopilot in this study. In any case, the point is that we must refrain from generalizations such as "headwind shears cause short landings". Headwind shears cause temporary loss of airspeed, lift, and control effectiveness, as described in this report. The resultant landing is dependent on the autopilot or pilot response to this condition.

The general recommendation evolving from this study is that performance in wind shear should be considered in automatic flight control system design, especially automatic flare. Systems using ground and airspeed inputs, and direct lift control are attractive candidates in this area. Because of the sensitivity of the landing parameters discussed in this report to airspeed errors, improved autothrottle control would probably be a significant factor in solving the wind shear problem. A parallel study to this one in the lateral axis, with vector shear, would likely identify similar problems.

BIBLIOGRAPHY

1. Chambers, E., "BOAC Experience with Turbulence," Paper #6, AGARD Conference Proceedings CP-140 on Flight in Turbulence, May 1973.

2. Snyder, C. T., "Analog Study of the Longitudinal Response of a Swept-Wing Transport Airplane to Wind Shear and Sustained Gusts During Landing Approach," NASA TN-D-4477, April 1968.

3. Luers, J. K., "A Model of Wind Shear and Turbulence in the Surface Boundary Layer," NASA CR-2288, July 1973.

4. Laynor, W. G. Jr., "Performance Study DCA-74-A-14," NTSB, Washington, D. C., July 1974.

5. Luers, J. K., and Reeves, "Effect of Shear on Aircraft Landing," NASA CR-2287, July 1973.

6. Trivett, L., "Design and Investigation of a Wind-Shear-Proof Control System for Automatic Landing," Thesis, AFIT, June 1973.

7. Houbolt, J. C., "Survey on Effect of Surface Winds on Aircraft Design and Operation and Recommendations for Needed Wind Research," NASA CR-2360, December 1973.

8. Lockheed Corp., Calif., "Improvement of Autoland Atmospheric Environment Models," LR 25615, December 1972.

9. Skelton, G. B., "Investigation of the Effects of Gusts on V/STOL Craft in Transition and Hover," AFFDL.

APPENDIX A

WIND MODELS

Logarithmic Shear

According to Luers (Ref 3), mean wind profiles depend on atmospheric stability, or the comparison of the temperature lapse rate with the adiabatic lapse rate. In the cases of stable air (temperature lapse rate < adiabatic lapse rate), unstable air (temperature lapse rate > adiabatic lapse rate), and neutral air (lapse rates approximately equal), the wind profile is a modified logarithmic curve. Only in strong inversions, where the temperature lapse rate is much less than the adiabatic lapse rate, does the profile assume a different shape. The atmosphere becomes discontinuous in this very stable air, and a steady wind changes abruptly at a given altitude, then remains constant or shears logarithmically.

Since the use for this model was only to show response trends in aircraft while landing, the model chosen for shear was a simple logarithmic equation. Luers' equation is:

$$\bar{u} = \frac{u^*}{K} \left[\ln \left(\frac{h}{h_o} \right) + \psi \left(\frac{h}{L} \right) \right]$$

where $\bar{u}$ = mean wind value

u^*, h_o = surface parameters

$\frac{h}{L}$ = stability parameter

K = von Karman constant

$$\psi\left(\frac{h}{L}\right) = \begin{cases} \text{linear function of } \frac{h}{L} & \text{(stable air)} \\ 0 & \text{(neutral air)} \\ \text{complex integral function } \frac{h}{L} & \text{(unstable air)} \end{cases}$$

This was limited for this study to only the neutral stability case:

$$\bar{u} = \frac{u^*}{K} \ln \left(\frac{h}{h_o} \right)$$

Since the surface parameters will vary depending on location, season, time, etc., arbitrary parameters were substituted for them in the shear equation

$$\bar{u} = C \ln \left(\frac{h}{h_o} \right)$$

Using the boundary conditions:

$$u = U_{IC} \text{ at } h = h_{SH} \text{ (nominally 500')}$$

$$u = U_f \text{ at } h = h_f \text{ (wheel height, 10')}$$

We can solve for the constants h_o and C. The final equation is:

$$u = \left(\frac{U_F - U_{IC}}{\ln h_f/h_{SH}} \right) \ln \left(\frac{h}{h_{SH}} \right) + U_{IC}$$

This equation was solved digitally in the simulation and sampled during approaches.

Knife-Edge Shear

No analytical expression was derived for the knife-edge shear. Instead, a "smoothed" step function was digitized and sampled from the function generator on the hybrid simulator. A step function passed through a lag would probably yield acceptable results as well.

APPENDIX B

AUTOMATIC FLARE SYSTEM

The block diagram of the flare system used for this study is shown in Figure 24.

The desired equations for the exponential flare are:

$$h = Ke^{-\frac{1}{\tau}t} - b \qquad \dot{h} = -\frac{K}{\tau}e^{-\frac{1}{\tau}t}$$

where b gives a final $\dot{h}$ touchdown bias. This is actually the solution to the differential equation:

$$\dot{h} + \frac{1}{\tau}h - \frac{b}{\tau} = 0$$

The constants can be determined by applying the boundary conditions. For an approach speed of 262 fps, on a 2.8° glideslope,

$$\dot{h}(0) = -12.8 \text{ fps}$$

$$h(0) = 60 \text{ ft} \quad \text{(arbitrary)}$$

$$h(t_f) = 0 \text{ ft}$$

$$\dot{h}(t_f) = -2.5 \text{ fps} \quad \text{(arbitrary)}$$

The fourth boundary condition is needed to determine t_f.

Solving for τ, K, t_f, and b yields

$$\tau = 5.83 \qquad K = 74.56$$

$$b = -14.56 \qquad t_f = 9.51$$

The proportional and integral gains used for the controller in the flare system were chosen based on a root locus analysis. The values were further refined to match the computer simulation response to that of the actual aircraft. The final values produce heavily damped modes with large gain margins.

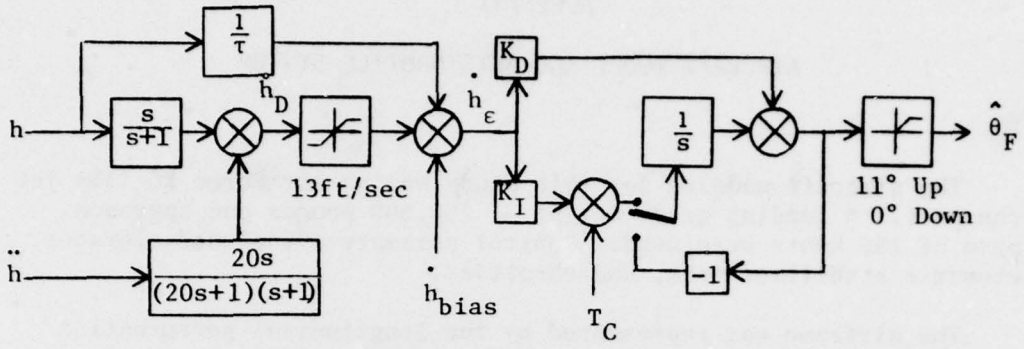

$\dot{h}_{bias}$ = touchdown sink rate bias = -2.5 ft/sec

K_D = proportional gain = .224

K_I = integral gain = .11

T_C = stab trim compensation = .40 deg/sec

τ = time constant = 5.83 sec

$\hat{\theta}_F$ = flare command

$\dot{h}_D$ = derived complimentary filtered $\dot{h}$

$$= \left[\frac{s}{s+1}\right] h + \left[\frac{20s}{(20s+1)(s+1)}\right] \ddot{h}$$

$$= \dot{h} \left[\frac{20s^2 + 20s + 1}{20s^2 + 21s + 1}\right]$$

$$\approx \dot{h}$$

$$\dot{h}_\varepsilon = \dot{h} + \frac{1}{\tau} h - \dot{h}_b$$

when $\dot{h}_\varepsilon = 0$

$$\dot{h} = \dot{h}_o e^{-\frac{1}{\tau} t} + \dot{h}_b$$

FIGURE 24. Automatic Flare System

APPENDIX C

AIRCRAFT MODEL AND AUTOTHROTTLE SYSTEM

The aircraft modeled for this study was an Air Force KC-135A jet transport. A landing gross weight of 160,000 pounds and approach speed of 155 knots were used. Control parameters included elevator, automatic stabilizer trim, and throttles.

The airframe was represented by the longitudinal perturbation equations of motion:

$$\ddot{\theta} = M_w w + M_{\dot{w}}\dot{w} + M_q\dot{\theta} + M_{\Delta T}\Delta T + M_{\delta e}\delta e + M_H H + M_{\delta s}\delta s$$

$$\dot{w} = Z_w w + Z_{\dot{w}}\dot{w} + (V+Z_q)\dot{\theta} + Z_u u + Z_{\delta e}\delta e + Z_H H$$

$$\dot{u} = -q\theta + X_w w + X_u u + X_{\Delta T}\Delta T + X_{\delta e}\delta e + X_H H$$

The parameter H is due to ground effect.

$$H = 1 - A/A_G$$

where A = Aspect ratio

A_G = Effective aspect ratio in the pressure of ground effect.

From a curve fit to empirical data

$$H = .0139\ e^{h'/30.68}$$

where $h' = 120 - h_{c.g.}$

The stabilizer surface, δ_s, responds to torque on the elevator servo motor. Since servo torque was not explicitly modeled in the simulation, a dead zone of stabilizer position was used. The trim rate was .15 deg/sec whenever elevator position exceeded .5 degrees from trim.

The elevator was modeled by a first order lag with a break frequency of 6 radians/sec. The throttles are separated into subsystems. The throttle servo is modeled as:

$$\frac{\delta_T}{\hat{\delta}_T} = \frac{1}{1+.1s}$$

The transfer function of throttle position to a change in thrust is modeled as:

$$\frac{\Delta T}{\delta_T} = \frac{75000}{1+6.67s} \quad \frac{lb}{deg}$$

For entry into flare, the aircraft flew autopilot coupled to a 2.7° glideslope.

The pitch autopilot responded to beam deviation damped by filtered altitude rate. Beam error was desensitized with respect to altitude to account for beam divergence as the aircraft approached the beam origin. Details of the autopilot are not included here since they are relatively unimportant to flare performance. (The beam gain was 0 by 80 feet AGL.)

The throttle system measured airspeed error (u_e), longitudinal acceleration ($\ddot{x}$) and filtered elevator position (δe) (for lead), using a 4 second gust filter on u_e and $\ddot{x}$. The control law used proportional plus integral control to maintain airspeed. At 110 feet, throttle movement was completely frozen, until 60 feet where it retarded linearly at 5°/sec to idle.

The throttle system block diagram is shown in Figure 25.

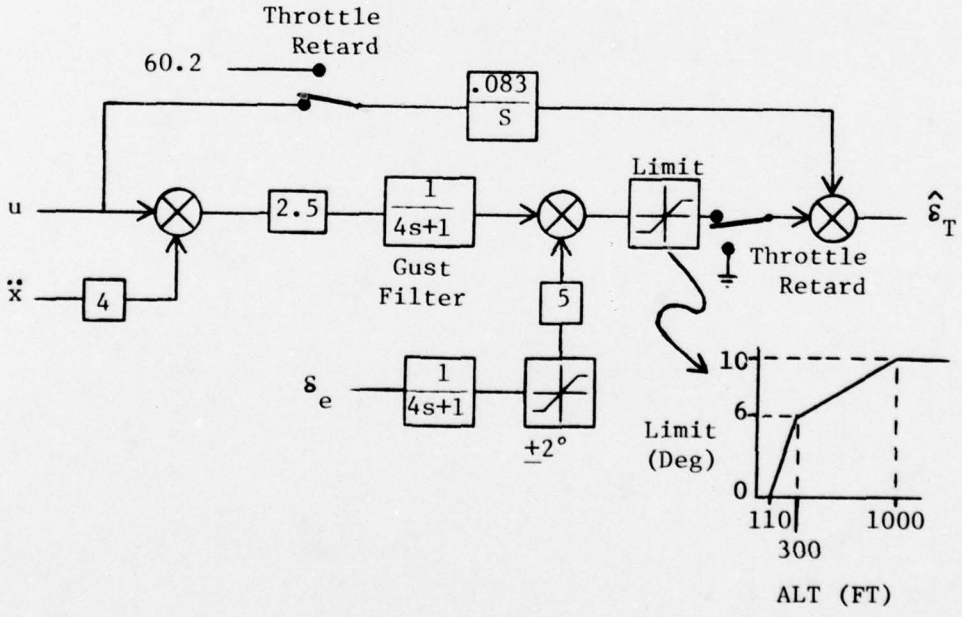

FIGURE 25. Autothrottle System

☆ U. S. GOVERNMENT PRINTING OFFICE: 1977 — 757-001/489